



3 1293 01766 5054

This is to certify that the
dissertation entitled
Investigation of carbohydrate recognition in
the developing nervous system of the leech.

presented by

Mei-Hui Tai

has been accepted towards fulfillment
of the requirements for

Ph.D. degree in Physiology


Major Professor

Date 10-14-98

**LIBRARY
Michigan State
University**

PLACE IN RETURN BOX
to remove this checkout from your record.
TO AVOID FINES return on or before date due.

DATE DUE	DATE DUE	DATE DUE
AUG 25 2008 07 08 09		

**INVESTIGATION OF CARBOHYDRATE
RECOGNITION IN THE DEVELOPING NERVOUS
SYSTEM OF THE LEECH**

By

Mei-Hui Tai

A DISSERTATION

**Submitted to
Michigan State University
in partial fulfillment of the requirements
for the degree of**

DOCTOR OF PHILOSOPHY

Department of Physiology

1998

ABSTRACT

INVESTIGATION OF CARBOHYDRATE RECOGNITION IN THE DEVELOPING NERVOUS SYSTEM OF THE LEECH

By

Mei-Hui Tai

Carbohydrate mediated interactions have been shown to play a crucial role in the development of the leech nervous system. This is of interest because carbohydrates have an enormous potential for encoding biological information and had therefore been considered ideal recognition molecules for the formation of precise connections between the vast number of neurons in a nervous system. While there is some evidence that carbohydrates on the cell surface membrane interact homotypically, most of their interactions, as was shown in systems other than the nervous system are heterotypic and involve carbohydrate-binding proteins or lectins.

Leech sensory afferents express a constitutive mannose-containing epitope on their cell surface that is recognized by monoclonal antibody Lan3-2. This mannose marker enables sensory afferents that enter the CNS as a tightly (fasciculated) bundled axon tract to defasciculate and arborize across the CNS neuropil (Zipser, et al., 1989). Sensory arbors were abolished by perturbing sensory afferents in the intact nervous system with Lan3-2 Fab fragments (Song and Zipser, 1995a). To understand the implications of mannose-specific recognition for synaptogenesis, we studied the effects of antibody perturbation at the ultrastructural level. Our observations suggest that sensory afferents

normally first branch into collaterals inside their CNS target region and then generate synaptic vesicle clusters in their expanding sensory trunks. Perturbing sensory afferents of their mannose-specific recognition leads to a loss of collateral branches and synaptic vesicle clusters.

Three leech galactose binding proteins (galectins) which may bind to these carbohydrates, have been isolated and characterized (Cole and Zipser, 1994a, b). These galectins with apparent molecular masses of 16, 35 and 63 kD are termed leech lectin 16, 35 and 63 (LL16, LL35, and LL63, respectively). LL16 and LL35 are endogenous to the leech's CNS, whereas LL63 is only present in peripheral organs. LL35 is highly expressed in a small subset of sensory afferent axons which project in the bilateral sensory midline tract of leech CNS. In this thesis, I characterized this subset of sensory afferents as photoreceptors by antibody staining and dye injections. I also identified one CNS neuron, the AP effector cell, as a likely postsynaptic partner for these sensory afferent neurons. Ultrastructural analysis confirmed that the nerve terminals of photoreceptors make direct contact with AP cell processes.

ACKNOWLEDGMENTS

First of all, I want to express my greatest thanks to my mentor, Dr. Birgit Zipser, for the years of guidance and encouragement that I had in her laboratory. Through day to day discussion, she helped me learn and excel the exciting field of Neurobiology research. I am forever thankful.

I want to thank my committee members, Drs. Steven Heidemann, Seth Hootman, Mary Rheuben, Ralph Pax and Connie Osborn, for their comments and advise throughout the research and writing process. In addition, I want to thank Drs. Steven Heidemann, Seth Hootman and Mary Rheuben for teaching me new techniques and allowing me to use their equipment.

I want to thank Dr. Richard Heisey and Burnell Selleck for their guidance and support during and beyond the semesters as a teaching assistant in PSL 431, 432. I also would like to thank Drs. John Heckman and Joanne Whallon for teaching me electron microscopy and Silicon Graphics Work Station, which I used most for my thesis work.

My gratitude also goes to my laboratory colleagues: Drs. Connie Osborn, Jonathan Song, Michelle Erhardt and Angela Chapman for their support and friendship. Many thanks to my fellow graduate students for their friendship and help from the secretarial staff in the Department of Physiology, especially, Dr. Chingju Lin and Sharon Shaft.

Last but most importantly, I want to express my million thanks to my husband and best friend, Feng-Jong Lee, for his love and support that made this work possible. To my beloved daughter Natalie, thanks for brightening up my days.

TABLE OF CONTENTS

LIST OF TABLES	vi
LIST OF FIGURES.....	vii
LIST OF ABBREVIATIONS.....	ix
INTRODUCTION.....	1
CHAPTER 1. Mannose-specific recognition mediates two aspects of synaptogenesis of leech sensory afferents: collateral branching and formation of synaptic vesicle clusters.	9
Introduction.....	11
Materials and Methods.....	14
Results.....	23
Discussion.....	49
CHAPTER 2. Identification of the sensory modality of the subset of sensory afferent which expresses a high concentration of leech galectin and identification of its potential postsynaptic partners.....	54
Introduction.....	56
Materials and Methods.....	58
Results.....	63
Discussion.....	87
SUMMARY AND CONCLUSIONS.....	93
LIST OF REFERENCES.....	95

LIST OF TABLES

Table 1.	Carbohydrate markers of leech sensory afferents.	6
Table 2.	Area measurement of ventral target region in control and perturbed embryos.	33

LIST OF FIGURES

Figure 1.	Determination of antibody concentration for staining sensory afferents in live embryos.	19
Figure 2.	The sensory afferent system of embryonic leech.	25
Figure 3.	Sensory afferents in control embryos and embryos cultured in Lan3-2 Fab fragments.	29
Figure 4.	Histogram comparing the number of branches and branchlets in control embryos and embryos cultured in Lan3-2 Fab fragments.	32
Figure 5.	Control sensory afferent trunk with synaptic vesicle clusters.	37
Figure 6.	Histogram comparing the amount of synaptic vesicle clusters in control embryos and embryos cultured in the presence of Lan3-2 Fab fragments.....	39
Figure 7.	Three-dimensional reconstruction of the processes of a sensory afferent in its target region.....	41
Figure 8.	Wire frame reconstruction of a control sensory afferent trunk with synaptic vesicle clusters.	43
Figure 9.	Schematic presentation of a sensory afferent in its target region.	46
Figure 10.	Schematic presentations of perturbed sensory afferents in an embryo cultured in Lan3-2 Fab fragments.	47
Figure 11.	The cell body and axon of a photoreceptor in leech eye are galectin immunoreactive.	65
Figure 12.	DiO injection of photodetectors.	69
Figure 13.	Colocalization of AP cell projection with sensory afferents.	73
Figure 14.	Colocalization of Retzius cell and N cell projections with sensory afferents.	75
Figure 15.	Optic neuropil and AP cell processes.	78

Figure 16. Magnified view of the region shown in the box in Figure 15.	81
Figure 17. Electron micrograph showing that AP projection contacts photoreceptors.	83
Figure 18. Electron micrograph showing that AP projection contacts somato-, chemosensory neuropil.	86

LIST OF ABBREVIATIONS

AP	anterior pagoda
BSA	bovine serum albumin
CE0	carbohydrate epitope 0, which contains mannose, is shared by the fullset of sensory afferent neurons. This epitope is recognized by mAb Lan3-2
CE1	carbohydrate epitope 1, which contains α -galactose, is expressed by a large subset of sensory afferent neurons. This epitope is recognized by mAb Laz 2-369
CE2	carbohydrate epitope 2, which contains both glucose and α -galactose, is expressed by a medium subset of sensory afferent neurons. This epitope is recognized by four different mAbs, among them Laz 7-79
CE3	carbohydrate epitope 3, which contains β -galactose, is expressed by a small subset of sensory afferent neurons. This epitope is recognized by mAb Laz 141
CNS	central nervous system
DAB	3,3'-diaminobenzidine
DiO	3,3'-dioctadecyloxycarbocyanine perchlorate; diO-C18-(3)
DMSO	dimethyl sulfoxide
EDTA	ethylenediaminetetraacetic acid
EGTA	ethyleneglycol-bis(beta-aminoethyl ether)N,N,N',N'-tetraacetic acid
EM	electron microscope

Fab	binding fragment of antibody generated by papain digestion
FITC	fluorescein isothiocyanate
GalNAc	N-acetyl-galactosamine
GOD	glucose oxidase
HEV	high endothelial venules
HRP	horseradish peroxidase
kD	kilodaltons
L-15	Leibovitz 15
Lectins	carbohydrate binding proteins
LL16	leech lectin 16
LL35	leech lectin 35
LL363	leech lectin 63
LM	light microscope
mAb	monoclonal antibody
MG	midbody ganglion
NCAM	neuronal cell adhesion molecules
PAGE	polyacrylamide gel electrophoresis
PBS	phosphate buffered saline
PSA	polysialic acid
SDS	sodium dodecyl sulfate
SSEA	stage-specific embryonic antigens
TX-100	Triton X-100

INTRODUCTION

Cells recognize one another through pairs of complementary structures on their surfaces: a structure on one cell carries encoded biological information that the structure on the other cell can decipher. Recognition is a central event in many biological phenomena and the first step in numerous processes in cell-cell interactions, such as fertilization, embryogenesis, bacterial infection and immune defense. Since about 1970 evidence has accumulated that cells express carbohydrates on their surfaces in the form of glycoproteins, glycolipids and polysaccharides (Jessell et al., 1990). Theoretically, carbohydrates make ideal recognition molecules because of their enormous potential for encoding biological information. In peptides and oligonucleotides, the information content is based only on the number of monomeric units and their sequence, whereas in carbohydrates, information is also encoded in the position and anomeric configuration (α or β) of glycosidic units and in the occurrence of branch points. For example, four amino acids can only encode 24 tetrapeptides while four monosaccharides can encode as many as 35,560 tetrasaccharides (Sharon and Lis, 1989; Sharon and Lis, 1993).

The carbohydrate moieties of proteins and lipids (glycoconjugates) interact with carbohydrate-binding proteins (lectins) in many non-neuronal recognition events. The stage- and species-specific binding of a sperm to the zona pellucida coat that surrounds mammalian oocytes has been shown to result from the interaction of sperm receptor with an O-linked oligosaccharide that is present on the zona pellucida glycoprotein, ZP-3 (Bleil and Wassarman, 1980; Wassarman, 1987). Studies of preimplantation mouse embryos have provided evidence for the role of both calcium-dependent adhesion

molecules and oligosaccharides in blastomere adhesion. The calcium-dependent cell adhesion molecule, E-cadherin, is expressed on blastomeres at the 8-cell stage and mediates the early, Ca^{2+} -dependent phase of developmental stage (Takeichi, 1986). The possibility that oligosaccharides are involved in blastomere adhesion derived initially from analysis of a set of lactoseries oligosaccharides, originally defined as stage-specific embryonic antigens (SSEA) (Solter and Knowles, 1978).

The adhesion of lymphocytes to a specialized set of high endothelial venules (HEV) in post-capillary beds (lymphocyte homing) appears to depend, at least in part, on receptors that recognize specific carbohydrate structures. Evidence has been shown that sialidase treatment of HEV cells perturbs lymphocyte adhesion (Rosen et al., 1985; Gallatin et al., 1986). Finally, the endocytosis of circulating serum glycoproteins by hepatocytes is also involved in carbohydrate recognition. It has been demonstrated in the rat, that the removal of terminal sialic acid residues from native serum glycoproteins exposes galactose residues and results in the accelerated clearance of these glycoproteins from the circulation (Ashwell and Harford, 1982).

In the nervous system, the complexity of cell interactions has made determination of the precise function of carbohydrates and lectins substantially more difficult than in non-neuronal systems. Within the nervous system, there is no direct evidence that carbohydrates subserve similar adhesion or recognition functions. Indirect support has been derived from the restricted expression of cell surface glycoconjugates and their potential carbohydrate binding proteins on subsets of neurons (Scott et al., 1990), growth cones (Pfenninger et al., 1984) and at synaptic sites (Scott et al., 1988). It suggests that

the surface glycoconjugates and carbohydrate-binding proteins may mediate many aspects of neuronal development or function. For example, biochemical support for the existence of carbohydrate gradients in the retino-tectal system in the chick embryo was originally obtained by measuring the adhesion of dissociated dorsal or ventral retinal cells to topographically appropriate tectal regions *in vitro*. A synapse-specific carbohydrate at the neuromuscular junction of rat skeletal muscle has been identified by labeling with a plant lectin, *Dolichos biflorus* agglutinin (DBA) that recognizes N-acetylgalactosamine (GalNAc) β -terminal saccharides (Sanes and Cheney, 1982; Scott et al., 1988).

However, it has proven difficult to determine the role of specific neuronal carbohydrate markers involved in the formation of neuronal connections, presumably because they are expressed on neurons only as long as the nervous system remains intact. Partially differentiated neurons in brain slices or neuronal cell lines lose their normal carbohydrate markers (Barakat et al., 1989; Oudega et al., 1992) and instead express anachronistic surface carbohydrates that can resemble those of undifferentiated neuroblasts.

Understanding the function of endogenous glycoconjugates and lectins in the nervous system would be facilitated by a model system that is less complex than the vertebrate nervous system and that is readily amenable to experimental manipulation. We used the virtually intact cultured leech embryos to study the normal function of carbohydrate markers in the development of nervous system.

Our laboratory has developed a culture system in which the germinal plate of leech embryos shows a rate of sensory afferent development that is 92% of the normal rate *in*

vivo. The superb sensitivity of sensory afferent neurons in response to the low concentration of perturbing reagent is able to delineate multiple, sequential steps of axonal targeting that are mediated via different carbohydrate recognition events.

The leech embryo provides a serial array of developmental time points due to the anterior to posterior developmental gradient of its 32 segments (Fernandez and Stent, 1982; McGlade-McCulloh et al., 1990). Each segment contains one CNS ganglion which is innervated by two bilaterally paired tracts of sensory afferent axons whose cell bodies are associated with epithelial layers. The cell bodies are located in a set of sensilla (clusters of sensory organs) lying on the middle annulus of each segment on the body wall and transduce different sensory modalities: mechano-, chemo-, heat-, and photo detection (Weisblat and Shankland, 1985; Zipser, 1994). The axons of sensory afferents project through peripheral nerves into the CNS. As in the vertebrate (Scott et al., 1990; Riddle et al., 1993), functional sets and subsets of leech sensory afferents can be distinguished by their different carbohydrate markers (Peinado et al., 1990). A group of 130 kD surface glycoproteins which are expressed on sensory afferent neurons and glia in the leech (*Haemopsis marmorata*, *Hirudo medicinalis*) have been characterized through the use of monoclonal antibodies (Zipser and McKay, 1981). The full set of leech sensory afferent neurons can be identified via a mannose-containing epitope, their generic marker carbohydrate epitope 0 (CE0) recognized by mAb Lan3-2. Disjoint subsets of these same neurons can be identified via three markers, CE1, CE2 and CE3 by different mAbs (Table 1). All of these neuronal markers are located on N-linked glycoconjugates of 130 kD surface proteins (Bajt et al., 1990; McGlade-McCulloh et al., 1990). Several lines of

indirect evidence exist that each of these carbohydrate encoded subsets transduce a particular sensory modality, e.g. mechano-, chemo-, and heat detection. The projections of sensory afferents undergo characteristic morphological changes during the formation of neuronal networks.

Previously, it had been shown that sensory afferents use their common mannose-containing marker, CE0, to defasciculate and arborize across their target regions in the CNS neuropil, the sensory neuropil (Peinado et al., 1987; Zipser et al., 1989). There are three lines of evidence that the first targeting step is mediated via a mannose-specific recognition. The defasciculation and arborization was inhibited by treating embryos with 1) Fab fragments that block the mannose-containing marker, 2) N-glycanase that cleaves N-linked carbohydrate chains on which the mannose-containing marker is located, and 3) multivalent-mannose in the form of neoglycoprotein, mannosylated bovine serum albumin (BSA) that competes for the putative receptors. In contrast, the expression of subset markers has the opposing role of restricting their respective neuronal subset into discrete subregions of sensory neuropil (Song and Zipser, 1995b). These results indicate that carbohydrate recognition events mediate the projections of sensory afferents in the leech central nervous system.

Table 1. Carbohydrate markers of leech sensory afferents

Sets or subsets	Epitopes	MAbs	Functions
Full set	CE0	Lan3-2	all sensory modalities
Large subset	CE1	laz2-369	putative mechanodectors
Medium subset	CE2	Laz7-79	putative chemodectors
Small subset	CE3	Lan2-3	putative heat detectors

Classically, carbohydrate recognition involves the interactions of carbohydrates with lectins. Animal lectins can be classified into two groups based on the structure of their carbohydrate-recognition domains and their requirement of calcium to maintain carbohydrate-binding activity (Drickamer, 1988; Kasai, 1990). Calcium-dependent lectins as a group recognize many specific saccharide structures and are widely distributed in vertebrates and invertebrates. In contrast, calcium-independent lectins (or S-type lectins) are specific for galactosides and were thought to be present only in vertebrates. However, calcium-independent lectins have been found in the nematode (Hirabayashi et al., 1996) and the sponge (Pfeifer et al., 1993). In the leech, three galactose binding lectins (galectins) have been isolated and characterized (Cole and Zipser, 1994a) with the apparent molecular weights of 16, 35 and 63 kD. These calcium-independent lactose-binding proteins are termed LL16 (Leech Lectin 16), LL35, LL63. Only LL16 and LL35 are present in the nervous system. Previous studies showed that LL35 is expressed by a small subset of sensory afferent axons which project in the bilateral sensory midline tract (Cole and Zipser, 1994b).

The principal goal of my thesis research is to further elucidate the role of carbohydrates and lectins in the development of the leech sensory afferent system using an ultrastructural approach. The first part of my research project is directed at studying the cellular mechanisms of sensory afferent development in the synaptic neuropil of the CNS at the ultrastructural level. The background for this ultrastructural work comes from extensive studies of this system at the light microscopic level: normally, sensory afferents expressing their constitutive mannose marker defasciculate and arborize as they enter the

CNS. Their projections extend separately through the neuropil. Perturbing their mannose marker with Fab fragments inhibits the defasciculation and arborization of sensory afferents. Instead, sensory afferents project as a fasciculated tract. It appears that the inhibition of mannose-specific recognition not only leads to the refasciculation of sensory afferent projections, but also to the loss of projections. To test this hypothesis and understand the implication of mannose-specific recognition for synaptogenesis, we studied the first targeting step of sensory afferents by using electron microscope. This work comprises Chapter 1 of this dissertation.

In the second chapter, I examined a subset of sensory afferents which expressed high levels of galectin. I showed that this sensory afferent subset is comprised of photodetectors. I also characterized possible monosynaptic connections between this subset of sensory afferents and their identified postsynaptic neurons. This work will lay the foundation for a future study directed at exploring the carbohydrate- and lectin-mediated developmental interactions at the single cell level.

CHAPTER 1. MANNOSE-SPECIFIC RECOGNITION MEDIATES TWO ASPECTS
OF SYNAPTOGENESIS OF LEECH SENSORY AFFERENTS:
COLLATERAL BRANCHING AND FORMATION OF SYNAPTIC
VESICLE CLUSTERS.

In the research described in this chapter, we studied the developmental role of carbohydrate markers in the genesis of neuronal networks using leech sensory afferents as a model. Leech sensory afferents express a mannose-containing epitope on their cell surface that is recognized by monoclonal antibody Lan3-2. Previously, the elaboration of central arbors in the synaptic neuropil of CNS ganglia was experimentally shown to depend on this mannose marker. Central arbors were abolished by perturbing sensory afferents in the intact nervous system with either Lan3-2 Fab fragments, a glycosidase, or mannose-BSA. To understand the cytological mechanism underlying mannose-specific recognition for synaptogenesis, we have now studied the effects of antibody perturbation at the ultrastructural level in the sensory afferent target region. A characteristic signature of a normal sensory afferent is its profuse collateral branching, which, with ongoing development, is replaced by a single widened process, the sensory trunk, that possesses numerous synaptic vesicle clusters. The inhibition of mannose-specific recognition leads to a rapid, major reorganization of sensory afferent growth. Collateral branches are fasciculated and resorbed, sensory trunks lose their synaptic vesicle clusters, and the pruned axons grow at an accelerated rate. These responses suggest that depriving sensory afferents of mannose-specific recognition aborts their synaptogenesis and causes them to resume behavior typical for tracking through axonal tracts. The current findings also

suggest that the mannose marker, by promoting both collateral branching and the formation of synaptic vesicle clusters, plays a critical role in two stages of sensory afferent synaptogenesis.

INTRODUCTION

Carbohydrate-mediated interactions via acidic or neutral glycans are being increasingly implicated in different stages of axonal targeting and synapse formation. Negatively charged carbohydrates such as sialic acid and the repeating disaccharide units of proteoglycans influence axonal targeting by providing anti-adhesive effects that vary with the cellular/molecular context of the neuronal environment (Rutishauser and Landmesser, 1996; Snow et al., 1991; Grumet et al., 1993; Faissner et al., 1994).

Neutral, galactose-containing glycans have been shown to promote different stages in the genesis of neuronal networks. For example, galactose-specific recognition not only mediates axonal targeting but also plays roles in later stages of synapse formation (Mahanthappa et al., 1994; Martin and Sanes, 1995; Song and Zipser, 1995b; Puche et al., 1996; Inoue and Sanes, 1997).

The interactions of mannose have been extensively documented outside the nervous system (Varki, 1993). Mannose is the neutral carbohydrate residue of oligomannosidic N-glycans prior to their processing and substitution with galactose and sialic acid (Kornfield and Kornfield, 1985). Evidence for the critical importance of mannose-specific recognition in neuronal development is now beginning to accumulate. For example, common oligomannosidic glycans, by mediating an interaction between L1 and NCAM, stimulate neurite outgrowth via signal transduction mechanisms (Horstkorte et al., 1993; Heiland et al., in press).

Using leech sensory afferents as a model system, we are addressing another function of mannosidic glycans, namely their role as cell-type specific markers. Leech sensory

afferents express an unusual mannose structure on N-linked carbohydrate chains of their 130 kD glycoproteins that is recognized by the monoclonal antibody Lan3-2 (Zipser and McKay, 1981; Peinado et al., 1990; Zipser et al., 1994). Recently, this mannosidic epitope was shown to be located on leechCAM and tractin, two common neuronal glycoproteins (Huang et al., 1997). Because the mannosidic epitope is a specific marker for sensory afferents, it appears to be a cell-type specific glycosylation of the common neuronal proteins.

The mannose marker of sensory afferents was shown to play a critical role in the growth behavior of sensory afferents as they enter the CNS. Arriving from the periphery in fasciculated tracts, they normally expand into central arbors as they enter the synaptic neuropil. The collapse of these central arbors is effected by three separate experimental manipulations which inhibit the interaction of the mannose marker (Zipser and Cole, 1991; Song and Zipser, 1994a).

We wished understand the nature of the cellular functions that are mediated by the sensory afferents' mannose marker. For example, does the collapse of central arbors result from the refasciculation or the resorption of processes? Do processes change in other ways, for example, make navigational errors or modify their rate of elongation? And finally, what are the consequences of inhibiting mannose-specific recognition for the cytoplasmic indicators of synaptogenesis in these sensory afferent neurons? We investigated these questions by examine the effects of Lan3-2 fab fragments at the ultrastructural level. Using quantitative electron microscopy and serial reconstruction of ultrathin sections, we here provide evidence that sensory afferents deprived of their

mannose-specific recognition cease to engage in synaptogenesis and instead regress to behavior suitable for elongating through axonal tracts.

MATERIALS AND METHODS

Breeding of embryos and preparation of germinal plates

All experiments were performed on individuals of the leech, *Hirudo medicinalis*, which were bred at room temperature (23°C) in diluted artificial sea water (Forty Fathoms [Marine Enterprises, Inc., Baltimore, MD]; 0.5 g/L distilled water) and fed with fresh bovine blood once a month. After isolation for 2 months at 15°C, adult leeches were brought together in pairs for mating for about 1 month at room temperature. Gravid leeches were then placed in plastic boxes containing moist sphagnum moss. Boxes were checked daily for cocoons. Once found (day 0), cocoons, each containing 12-18 sibling embryos of the same age, were transferred to an incubator at 20°C. For experiments, the epithelial envelope of embryos was cut dorsally to extrude yolk and expose the ventral germinal plate, which was then stretched out by pinning the cut edges of the epithelial envelope against Sylgard-coated (184 silicon; Dow Corning Co., Midland, MI) culture dishes (35 X10 mm)(Corning Glass Works, Corning, NY). Embryos were cultured at 20°C in 1 mL of a defined growth medium consisting of Leibovitz-15 (L-15; Gibco, Grand Island, NY) with 1% ITS⁺ (Collaborative Research, Bedford, MA), 1 nM nerve growth factor (Sigma, St. Louis, MO), 10 nM epidermal growth factor (Collaborative Research), and supplemented with 10 mM KCl.

Monoclonal antibodies and their Fab fragments

The antibodies used in this study were generated by our laboratory. Lan3-2 is a monoclonal antibody (mAb) that binds to the full set of peripheral sensory afferent

neurons (Zipser and McKay, 1981; Zipser, 1994). Conjugation of horseradish peroxidase (HRP, Boehringer Mannheim, Indianapolis, IN) to mAb Lan3-2 was performed according to the glutaraldehyde coupling method of Avrameas and Ternynck's (Avrameas and Ternynck, 1971). In this two step method, 10 mg of HRP was first dissolved in 0.2 ml of 100 mM sodium phosphate (pH 6.8) containing 1.25% glutaraldehyde (Sigma, St. Louis, MO). After 18 hr at room temperature, excess free glutaraldehyde was removed by gel filtration (Sephacryl S-300 gel matrix, Pharmacia, Piscataway, NJ). Fractions containing the active enzyme were first pooled and concentrated to 10 mg/ml (1ml final volume) by ultrafiltration (Centricon-10, Amicon, Beverly, CA), and then the sodium chloride buffer was replaced with 100 mM sodium carbonate-bicarbonate (pH 9.5) by washing the ultrafiltration membrane. About 0.1 ml of mAb Lan3-2 (5 mg/ml in 0.15 M NaCl) was added to the enzyme solution and the pH of the solution was adjusted to > 9.0. The mixture was incubated at 4°C for additional 24 hr. The coupling reaction was quenched by adding 0.1 ml of 0.2 M ethanolamine (pH 7.0) and the mixture was incubated for another 2 hr at 4°C. To test the success of the coupling reaction, live juvenile nerve cords were incubated overnight in different titrations of the HRP-conjugated mAb Lan3-2 solution, then rinsed and processed for the DAB (3,3'-diaminobenzidine, Sigma) reaction. The stained nerve cords were embedded in Permount (Fisher Scientific Co., Fair Lawn, NJ) and checked under the light microscope.

Fab fragments were prepared from Lan3-2-containing ascites fluid that had been ammonium sulfate precipitated, digested with mercuripapain, and subjected to ion-exchange chromatography. The concentration of Fab fragments per fraction was estimated, assuming that 1 mg/mL of immunoglobulin has an absorption of 1.4 at 280

nm. The protein concentration was also determined using a Coomassie blue binding assay (Bradford, 1976). As determined on silver-stained SDS-polyacrylamide gels, Lan3-2 fab fragments had a molecular weight of 55 kD.

Perturbation experiments

The germinal plates of sibling embryos of a given cocoon were divided into three groups, each containing at least three siblings which were: 1) immediately stained after dissection, 2) used as controls, and 3) used for experimental treatments.

The germinal plates of both the control and experimental embryos were cultured for 6 hr in defined medium prior to the perturbation experiment. Previously, we determined that it takes 6 hr for sensory afferents to resume their normal rate of differentiation after dissection and that during these initial 6 hr, sensory afferents are less sensitive to the perturbing antibody (Song and Zipser, 1995a). After the pre-conditioning, experimental embryos were exposed to culture medium containing Lan3-2 Fab fragments (50 nM) for a duration of 3 hr while the medium of the control embryos was replaced only with fresh defined medium.

After rinsing, live control and experimental embryos were stained for 90 min with low concentrations of HRP-conjugated Lan3-2 antibody. Live rather than fixed tissue was stained because antibody penetration of fixed embryos requires detergent, which is detrimental to ultrastructural preservation. To arrive at a concentration of antibody that does not elicit appreciable perturbation effects, we compared the staining of control embryos (after 9 hr of culturing) to that of immediately stained embryos. We decreased

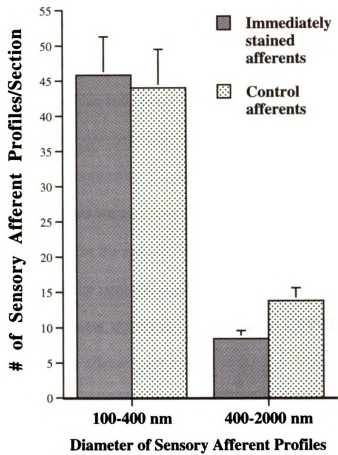
the titer of staining antibody until the frequency of collaterals and branchlets counted in both embryos was virtually the same (Figure 1).

Immunocytochemistry and sample preparation

All sibling embryos were fixed with 2% glutaraldehyde in L-15 medium for 30 min. To enhance the HRP-conjugated Lan3-2 staining, embryos were processed by the cobalt-glucose oxidase (Co-GOD) method. The procedure of the Co-GOD method was as follows: after washing briefly twice with 0.1 M cacodylate buffer (pH 7.4), embryos were placed in a 0.5% solution of CoCl₂ in 0.1 M cacodylate buffer (pH 7.4) for 10 min at room temperature. After washing three times with buffer, subsequently, the embryos were incubated for 60-120 min at 37 °C in a freshly prepared medium composed of 0.5 mg of DAB, 2 mg of β-D-glucose, 0.4 mg of NH₄Cl, 3 mg of GOD (Sigma, 34 U/mg) and 1 ml of 0.1 M cacodylate buffer (Itoh et al., 1979). After rinsing, ganglia were post-fixed with 1% osmium tetroxide (Ted Pella, Inc., Redding, CA) for 2 hr, dehydrated with serial changes of alcohol, and then transferred into propylene oxide (Polysciences, Inc., Warrington, PA) to be finally embedded in English araldite resin (Polysciences, Inc.). Ultrathin sections were cut on a LKB Ultratome V, collected on copper slot grids and stained with 10% uranyl acetate and Reynold's lead citrate. Grids were examined with a Philips CM10 electron microscope at 100kV.

Figure. 1 Determination of antibody concentration for staining sensory afferents in live embryos.

Sensory afferents were perturbed with Fab fragments of the same Lan3-2 monoclonal antibody that was used for their staining. To determine the concentration of staining antibody and the duration of exposure to the staining antibody that evoke minimal perturbations, we made use of our previous finding that sensory afferent growth is not appreciably perturbed by Fab fragments in the embryonic germinal plate immediately after it is put into culture; it takes a six hour preincubation for sensory afferents to resume normal differentiation in the cultured germinal plate and to become optimally sensitive to antibody perturbation (Song and Zipser, 1995a). One groups of embryos (immediately stained sensory afferents) was exposed to HRP-conjugated Lan3-2 after dissection while another group consisting of age-matched siblings was first cultured for 9 hr before exposure to HRP-conjugated Lan3-2. In our perturbation experiments, embryos cultured for 9 hr prior to staining served as controls for embryos perturbed by Lan3-2 Fab fragments. Both groups of embryos were fixed in glutaraldehyde, reacted with DAB and glucose oxidase, and processed for electron microscopy. Sensory afferent profiles with diameters of 100-400 nm (branchlets), and diameters of 400-2000 nm (collaterals) were counted in the two most posteriorly innervated midbody ganglia (MG 17 and 16) at level 2 of the ventral target region (see Figure 3). The concentration of staining antibody and the duration of staining were reduced until immediately stained and control embryos exhibited a comparable number of branchlets and collaterals as presented in this histogram. Results represent means \pm SE of 8 and 16 hemiganglia, from immediately stained and control embryos, respectively, each hemiganglion providing 5 samples.



Data analysis of the collateral branching of sensory afferents in control and perturbed embryos

To study the branching patterns of sensory afferents, we examined five different levels of the anterior aspect of the two most recently innervated CNS ganglia [Midbody ganglia (MG) 17, 16]. Level 1 was defined as the anterior-posterior level where the sensory afferents project through the roots and enter the ganglion. Level 1 was approached by cutting 1- μ m-thick sections from the posterior ganglion towards the root. Thick sections were stained with toluidine blue and checked under the light microscope in order to see the root structure. When the root region had been reached (level 1), twenty ultrathin sections were cut for later examination. To reach level 2, four thick sections were cut. Next, twenty ultrathin sections were cut and put on 4-5 grids. This procedure was repeated from level 3 to 5. For the analysis of branching, only one section/grid was examined in order to minimize sampling a given profile on two immediately adjacent sections. Sensory afferents were identified by DAB reaction product on their cell surface. In MG16 and MG17 sensory afferent profiles have diameters between 100 to 2000 nm. We analyzed the antibody perturbation by constructing a histogram of diameters (200 nm bin width) and found a bimodal distribution (100 - 400 nm, >400 nm). We refer to the smaller diameter group as branchlets and the larger diameter group as branches. All tests of statistical significance of perturbations were performed by Student's t test (two tailed).

Measurement of synaptic vesicle clusters

Synaptic vesicle clusters in sensory afferent profiles were measured in MG 14 which contained larger profiles (greatest diameter >2000 nm) than those seen in MG 16 and MG17. These large profiles were termed sensory trunks. Synaptic clusters occur in both sensory trunks as well as in the larger branches. Therefore, we included into this analysis branches with a minimum cross-sectional area of $0.25 \mu\text{m}^2$. Because profiles can have either round or ovoid shapes, we approximated their cross sectional area by multiplying their shortest and longest diameters. Before counting synaptic vesicle clusters, we reconstructed separate profiles of trunks and large branches using serial sections. Next, we counted the synaptic vesicle clusters separately for each reconstructed profile. Synaptic vesicle clusters often extended for several sections. To avoid the errors involved in volume reconstruction (Ungersbock et al., 1991), we estimated the summed areas occupied by synaptic vesicle clusters/profile in the different sections analyzed. To measure the area of a given synaptic vesicle cluster, the area was first outlined and then scanned into the computer. The area of the synaptic vesicle cluster was calculated using the area measurement function of the NIH image program. For each reconstructed profile, the synaptic vesicle area of its individual sections was summed. To obtain the normalized value for the area occupied by synaptic vesicles per section, the summed areas of the synaptic vesicle clusters were divided by the number of sections. Determining the synaptic area separately for each profile avoided errors due to the different degrees of branching of control and experimentally manipulated sensory afferents.

Three dimensional reconstruction

To obtain a more comprehensive view of sensory afferent structures, serial sections were cut and analyzed in both control and perturbed embryos. The longest series (100 ultrathin sections) obtained from the control embryo was also used for three dimensional reconstruction using a Silicon Graphics workstation at the Michigan State University Laser Scanning Microscope Laboratory. The surface membranes of trunks, collaterals and branchlets of a given neuron were manually traced and scanned into a Hewlett Packard scanner. During the tracing process, electron micrographs were aligned manually according to three fiducial marks. The regions of synaptic vesicle clusters were also traced and included in the profile structure.

RESULTS

Developmental age of the sensory afferents for the study of early synaptogenesis in CNS ganglia

After one-fourth of leech embryogenesis is completed, the cell bodies of sensory afferents differentiate in sensory organs called sensilla that are associated with the ventral epidermis. Sensory afferent cell bodies project their axons into their respective segmental CNS ganglia, 32 of which comprise the leech nerve cord. To study early stages in sensory afferent synaptogenesis, we made use of the anterior (first to develop) to posterior (last to develop) gradient by which sensory afferents differentiate in the embryonic leech. In the 10.5 day old embryos chosen for this study, sensory afferents have innervated 17 of the midbody CNS ganglia (MG). The four most recently innervated CNS ganglia (MG 17-14) are only supplied by sensory afferents arising from sensilla 3 in the ventral epidermis. Control and experimental embryos are grown in culture according to our previously developed method which permits the spatio-temporal gradient of sensory afferent development to proceed at 92% of its normal rate (Song and Zipser, 1995a).

To measure sensory afferent development in recently innervated ganglia at comparable anterior-posterior levels in the synaptic neuropil, we mapped the anterior aspect of the neuropil into five levels, separated by 5.6 microns each. At level 1, sensory afferents enter the CNS ganglia via the roots and bifurcate, changing their direction of growth by 90 degrees. At levels 2 to 5, sensory afferent growth is directed anteriorly (Figure 2A).

Figure 2. The sensory afferent system.

A) A schematic drawing of the sensory afferent system. The cell body of the sensory afferent which is associated with the epithelial layer of the skin projects its axon via peripheral pathways (a distance of 100 μm) into its segmental CNS ganglion to innervate its target region (VT) (indicated by hatching in the anterior aspect of the hemiganglion). For comparison across different ganglia, we have mapped the anterior ganglionic aspect into 5 levels, each separated by 5.6 μm . At level 1, the sensory afferent enters the ganglion, bifurcates and projects into the ventral target region. Projecting anteriorly, the sensory afferent elongates through its target region in parallel to the ganglionic midline (levels 2 to 5). At later developmental stages (not shown here), the sensory afferent will exit its target region to project into the connective, a central fiber tract, in order to innervate sensory afferent target regions in more anterior CNS ganglia. Likewise, the posterior limb of the sensory afferent will innervate more posterior CNS ganglia.

B) Schematic drawing of an EM micrograph showing a transverse section of a full ganglion at level 2. The box labeled C represents the area of the micrograph shown in C. The box labeled VT represents the area of the ventral target region which includes three fascicles with large profiles as well as numerous dispersed thinner profiles (indicated by shading). The arrow points to the fascicle whose large sensory trunk is pointed at by an arrow in C.

C) The low power electron micrograph shows a transverse section from an embryonic CNS ganglion (MG14, first innervated 21 hr ago) at level 2. Cell bodies of central neurons (S) surround the embryonic neuropil with its characteristic loosely arranged processes. The ventral target region of sensory afferents is located at the ventro-lateral aspect of the neuropil. Sensory afferents are only lightly stained with Lan3-2 to minimize eliciting perturbation effects during staining (see methods and Figure. 1). A wide sensory afferent profile which we call “trunk” is indicated (arrow). Calibration bar=2 μm .

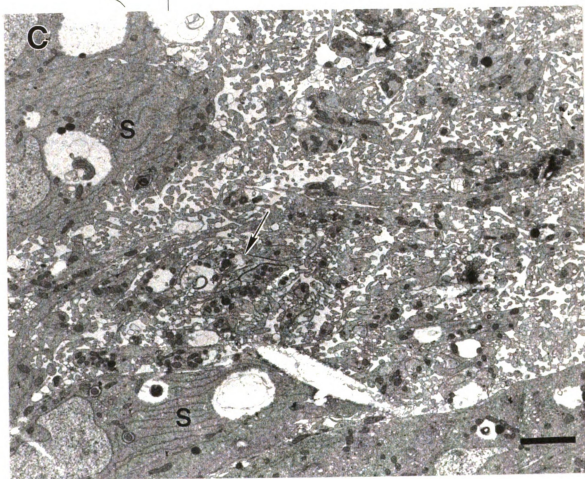
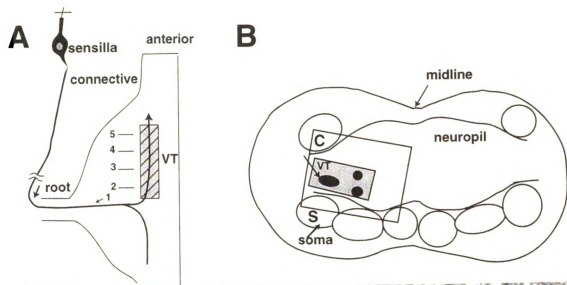


Figure 2B and C show a transverse section from an embryonic CNS ganglion taken at level 2, as a schematic presentation and a micrograph. Cell bodies (S) of central neurons surround the embryonic neuropil with its characteristic, loosely organized processes. The processes of sensory afferents are lightly stained for their mannose-containing surface marker with monoclonal antibody Lan3-2, using low antibody concentrations to minimize eliciting perturbation effects during staining (see Methods and Figure 1). The stained trunk of a sensory afferent neuron (Figure 2C, arrow) is visible in the central neuropil. Our ultrastructural studies showed that in recently innervated ganglia (MG17 - MG14, 10.5 d embryo), sensory afferents grow along the ventro-lateral aspect of the synaptic neuropil. Thus, of the four sensory afferent target regions found in the adult (ventral, dorsal and two medial target regions), sensory afferents first innervate their ventral target region (VT).

Antibody perturbation of sensory afferent branching

Previously, we studied the molecular mechanisms that mediate the branching of sensory afferents into central arbors at the light level, using three independent perturbation agents; Lan3-2 Fab fragments which block the mannose marker; N-glycanase which cleaves the mannose marker; and a neoglycoprotein (mannose multivalently conjugated to BSA) which competes for the putative mannose-binding protein. Inhibiting mannose-specific recognition with any of the above three reagents led to the disappearance of their central arbors, which were replaced by thin, fasciculated tracts (Song and Zipser, 1995a; Zipser and Cole, 1991; Zipser et al., 1989). Here we analyzed this perturbation of sensory afferent growth at the ultrastructural level to determine

whether the disappearance of central arbors is due to the fasciculation of sensory afferent processes or to the resorption of these processes, or to both fasciculation and resorption.

To analyze the function of the mannose marker using ultrastructural analysis, we perturbed sensory afferent growth with Lan3-2 Fab fragments. Age-matched sibling embryos from the same cocoon were cultured for three hours either in defined medium (control embryos) or in defined medium to which Fab fragments (50 nM) were added (experimental embryos). This protocol was expected to produce less than a 50% perturbation effect according to our previous measurements at the light level (Song and Zipser, 1995a). The rationale for using this protocol was to capture single sensory afferents at various degrees of perturbation, providing data to make inferences on the perturbation process. After culturing, the projections of sensory afferents were visualized by staining with antibody Lan3-2.

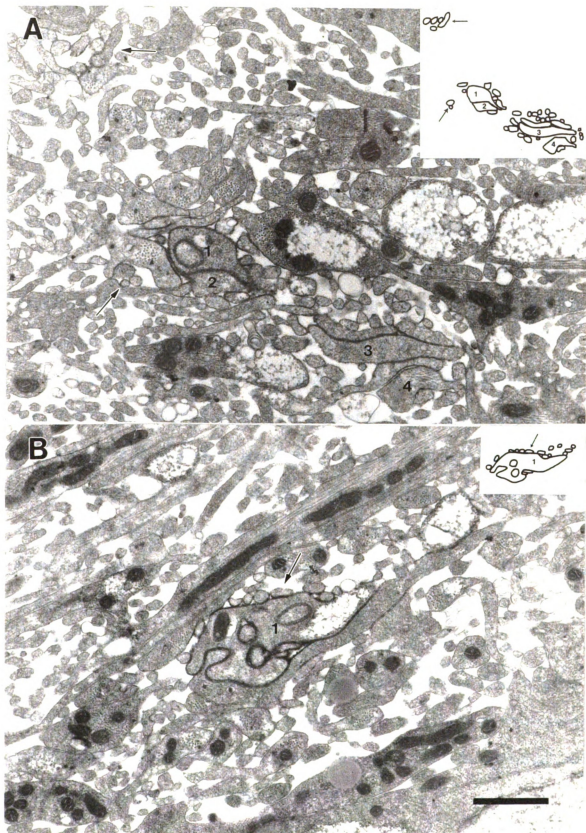
The ventral target region of a control embryo at level 2 of MG17 (Figure 3A) shows four sensory afferent profiles growing in three loosely separated fascicles that are surrounded by finer branchlets. Some sensory afferent branchlets project at a considerable distance from the larger profiles (arrows). There is also a profusion of unstained branchlets belonging to central neurons. The abundance of branchlets and the loose organization of the neuropil tissue is a characteristic feature of these early embryonic ganglia. A comparable aspect of the target region from an experimental sibling embryo cultured in Lan3-2 fab fragments is shown in Figure 3B. Here the target region contains only a single large sensory afferent profile that is surrounded by only a few branchlets. In embryos cultured in Lan3-2 Fab fragments, branchlets (arrow) are

Figure 3. Sensory afferents in control embryos and embryos cultured in Lan3-2 Fab fragments.

The electron micrographs show collateral growth of sensory afferents consisting of branches and branchlets in the ventral target region of the most recently innervated CNS ganglia (MG 17). The sensory afferents were stained in live embryos by HRP-conjugated Lan3-2 which binds to the mannose marker on their cell surface. The inserts are schematic presentations of sensory afferents within the given micrograph.

A) In the control embryo, the ventral target region consists of sensory afferents that project in a loose fascicle containing four branches (diameters: 400 - 2000 nm). Some of the thinner branchlets (n = 29; diameters: 100 - 400 nm) surround the branches. Others branchlets (n = 7) project as two clusters (arrows) at some distance away from the branches.

B) In an embryo cultured in Lan3-2 Fab fragments, the ventral target region consists of a single profile with the diameter assigned to branches. Branchlets (n = 18) project in the vicinity of the branch. All (arrow) except four of the branchlets project in a tight association with the branch. Calibration bar=1 μ m.



typically closely apposed to the thicker profiles or even invaginated into the thicker profile.

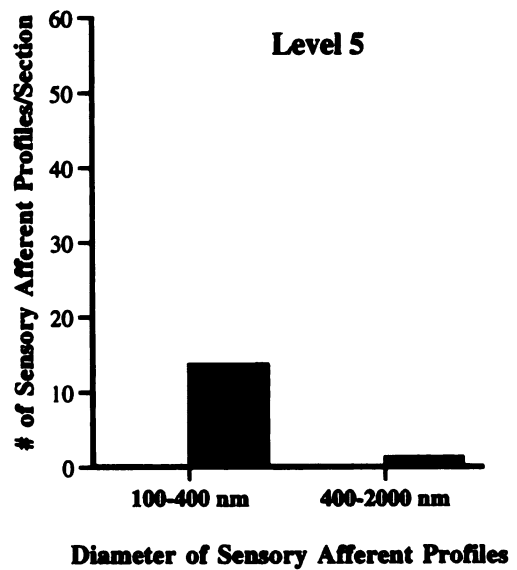
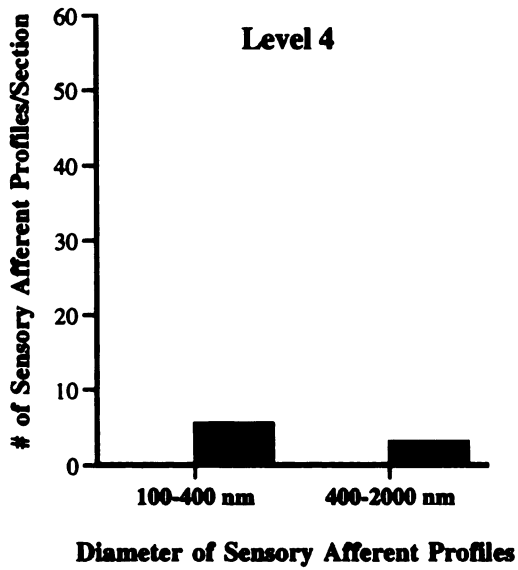
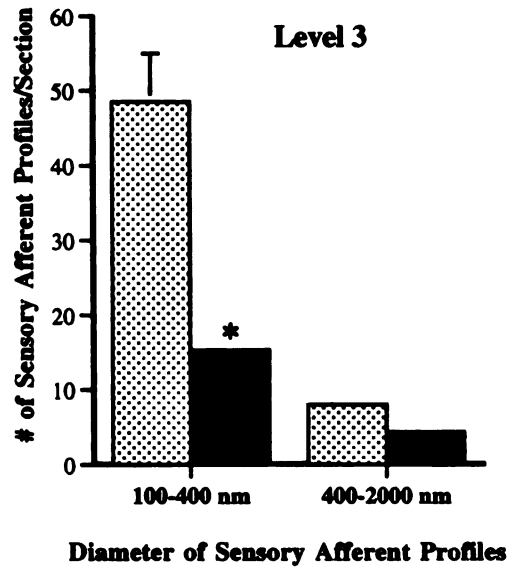
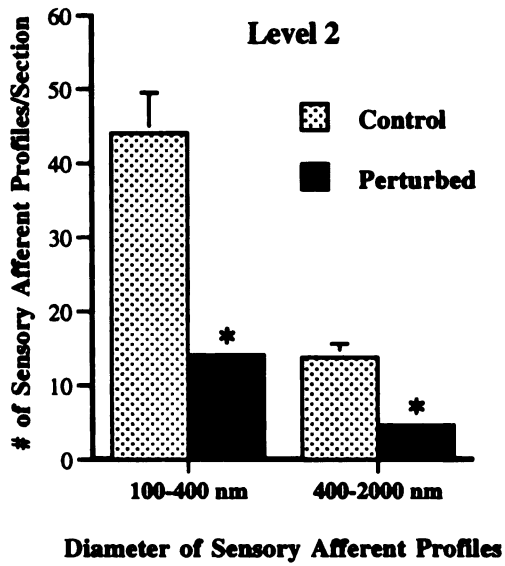
To quantitatively compare sensory afferent growth in control and experimental embryos, the frequencies of collaterals, separated into branches (400 - 2000 nm) and branchlets (100 - 400 nm), were counted in age-matched sibling embryos in three different experiments in a total of four control and four experimental sibling embryos. Collaterals were counted in the two most recently innervated ganglia (MG 17, 16) at levels 2 to 5, each ganglion providing two samples, because right and left halves of a ganglion are independently innervated by afferents from right and left sensilla 3 (control hemiganglia n=16; age-matched perturbed hemiganglia n=16).

At level 2, the proximal aspect of the target region, embryos grown in the presence of Lan3-2 Fab fragments demonstrate a four fold loss of all profiles, both the thicker branches and the finer branchlets, as compared to the control embryos (Figure 4). Likewise, at the level 3, the more distal aspect of the target region, there are four-fold fewer branchlets in the perturbed embryo compared to the control embryo. In both control and experimental embryos, the number of thick branches is smaller at level 3 than at level 2.

The perturbation effect elicited by Lan3-2 fab fragments could also be seen by comparing the areas of synaptic neuropil occupied by the ventral target region in control and perturbed embryos at levels 2 and 3. In control embryos, the area over which sensory afferent profiles are distributed was three- to four-fold larger than in the embryo cultured in the presence of Lan3-2 Fab fragments (Table 2).

Figure 4. Histogram comparing the number of branches and branchlets in control embryos and embryos cultured in Lan3-2 Fab fragments.

Branches (diameters: 400 - 2000 nm) and branchlets (diameters: 100 - 400 nm) of sensory afferents were counted in electron micrographs from the two most recently innervated CNS ganglia (MG17, 16) of control embryos and embryos cultured in the presence of Lan3-2 Fab fragments. Profiles were counted at levels 2 to 5 which represent posterior (proximal) and anterior (distal) aspects of the sensory afferent target region. Because most of the errors bars are too small to be visible at the scale at which the histograms are presented, we list them here: Level 2, perturbed embryo: branchlets and branches, 14.07 ± 0.87 and 4.62 ± 0.39 , respectively; level 3, perturbed embryo: branchlets and branches, 15.32 ± 0.80 and 4.32 ± 0.38 , respectively; level 4, branchlets and branches, 5.85 ± 0.56 and 3.15 ± 0.22 , respectively; level 5, branchlets and branches, 13.67 ± 0.88 and 1.33 ± 0.33 , respectively. Significantly different than control (*, $P < 0.001$). Results represent means \pm SE of 16 hemiganglia from the control and 16 hemiganglia from experimental embryos, each hemiganglion providing 5 samples.



	Target Region of Control Afferents (μm^2)	Target Region of Perturbed Afferents (μm^2)	P
Level 2	18.4 \pm 3.1	4.8 \pm 0.4	<0.001
Level 3	15.0 \pm 6.1	5.3 \pm 0.4	<0.001
Level 4	-	3.8 \pm 0.6	
Level 5	-	3.5 \pm 1.3	

Table 2. Area measurement of ventral target region in control and perturbed embryos. The ventral target region of sensory afferents in recently innervated CNS ganglia has an approximately rectangular shape in transverse sections of the neuropil. The size of this rectangular target region was estimated by multiplying its longest and shortest diameters. Ventral target regions were measured in 16 hemiganglia (MG17 and 16) at levels 2 to 5. The values are represented as means \pm SE. No valid P values can be computed for levels 4 and 5 (Sokal and Rohlf, 1981).

Antibody perturbation of the rate of sensory afferent elongation

Comparing sensory afferent development in the most recently innervated ganglia of control and experimental embryos also indicates that exposure to Lan3-2 Fab fragments affects the rate of sensory afferent elongation. In control embryos, sensory afferent processes only innervated the more proximal aspect of their target region, namely levels 2 and 3. In contrast, in the experimental embryos, sensory afferent processes also innervated the more distal aspect of their target region, the levels 4 and 5 (Figure 4).

The observation that sensory afferent processes reach into more distal aspects of their target region in experimental embryos compared to their control siblings indicates that depriving sensory afferents of their mannose-specific recognition leads to an acceleration of their growth rate. This accelerated growth occurs along the ventro-lateral aspect of the neuropil, within the ventral tract (VT), their proper target region. Thus, accelerated sensory afferent growth due to disrupting mannose-specific recognition is not accompanied by navigational errors.

The most distally innervated regions, level 5 in experimental embryos and level 3 in control embryos, possess the highest percentage of branchlets. As described below, with respect to the reconstructed sensory afferents, collateral branching is always richest at their distal growth regions.

Antibody perturbation of the formation of synaptic vesicle clusters

Analyzing embryos grown in Lan3-2 Fab fragments at the ultrastructural levels permits us to investigate possible perturbation effects on cytoplasmic indicators of synaptogenesis, e.g. the formation of synaptic vesicle clusters. In the two most recently

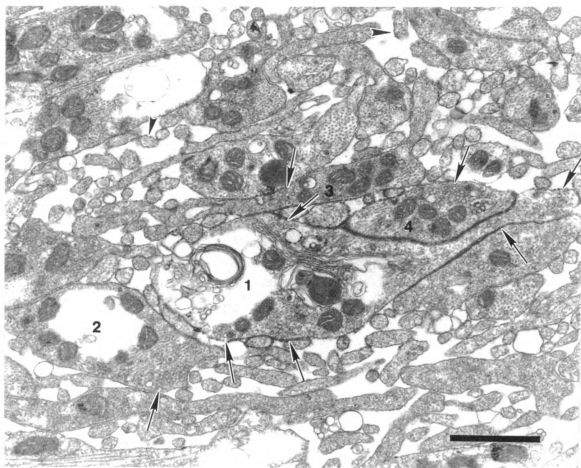
innervated ganglia (MG17 and MG16), there is a paucity of synaptic vesicle clusters in the sensory afferent profiles in both control and experimental embryos. In contrast, in MG14 of these same embryos synaptic vesicle clusters are present in sensory afferent profiles. MG14 is innervated 18 hr earlier than MG17.

A high power view of the ventro-lateral aspect of the synaptic neuropil of the control embryo (Figure 5) from MG14 (level 2) illustrates a fascicle with four sensory afferent profiles. Two of these profiles (>2000 nm) are larger than were seen in MG17 and 16, we call them sensory trunks (1, 2). The other two large profiles are considered to be branches (3, 4). In this section, trunk 1 possesses five clusters containing clear core synaptic vesicles. In addition to clear vesicles, this sensory trunk also has dense core vesicles (asterisks). The numerous mitochondria seen in the two trunks and large branches are further evidence that these profiles are developing into presynaptic regions.

To determine the effect of antibody exposure on the formation of synaptic vesicle clusters, we counted synaptic vesicle clusters in serially reconstructed trunks and branches of sibling embryos cultured in the absence and presence of Lan3-2 Fab fragments (Figure 6). We included only branches of a minimum size (minimal estimated cross-sectional area of $0.25 \mu\text{m}^2$) because the frequency of synaptic vesicle clusters drops off significantly as branches thin out.

To compare the distributions of synaptic vesicle clusters in control and experimental embryos, we summed the areas with synaptic vesicles in the serial sections of trunks (two trunks in the control embryo and four trunks in the perturbed embryo) and collaterals (two collaterals in the control embryo and three collaterals in the perturbed embryo), and

Figure 5. Control sensory afferent trunk with synaptic vesicle clusters. The micrograph shows a sensory afferent fascicle in a CNS ganglion that had been innervated for 21 hr (MG 14). It is a high-power view of the micrograph shown in Figure 2C. The fascicle consists of two trunks (1, 2) and two branches (3, 4). All profiles show synaptic vesicle clusters (arrows), dense core vesicles (asterisks) and mitochondria. Trunk 1, which has five synaptic vesicle clusters, belongs to the reconstructed neuron shown in Figures 7 and 8. Two branchlets projecting at a distance to the trunks and branches are pointed out with arrow heads. Calibration bar=1 μ m.



divided the sum by the number of sections. We did not attempt to measure the perturbation effect using volume reconstruction of these synaptic vesicle clusters because differences in section thickness can introduce error (Ungersboeck et al., 1991). Because each profile, trunk or branch, constitutes a separate sample, our comparison of synaptic vesicles in control and experimental afferents is independent of the number of processes that a given neuron possesses. As seen in Figure 6, there is six-fold reduction in the area of synaptic vesicle clusters in both trunks and branches of perturbed embryos compared to control embryos.

Reconstruction of a control sensory afferent

To better understand the impact of mannose-specific recognition and its inhibition on the three dimensional distribution of processes and their synaptic vesicle clusters, we reconstructed sensory afferents in MG 14 and MG17. One of the four sensory afferents reconstructed from MG14 of the control embryo is shown in Figures 7, 8 and 9. The processes of this sensory afferent, shown as a solid reconstruction in Figure 7, were reconstructed from 100 serial sections (an estimated distance of 8 μm). To facilitate viewing the profuse collateral growth of this neuron, it is presented in five different segments stacked on top of each other. The trunk region of this sensory afferent was also reconstructed using a transparent 'wire frame' method to illustrate the number and distribution of its synaptic vesicle clusters (Figure 8). In the accompanying drawing (Figure 9), the three dimensionally projecting processes of this neuron are schematically presented in the two-dimensional plane.

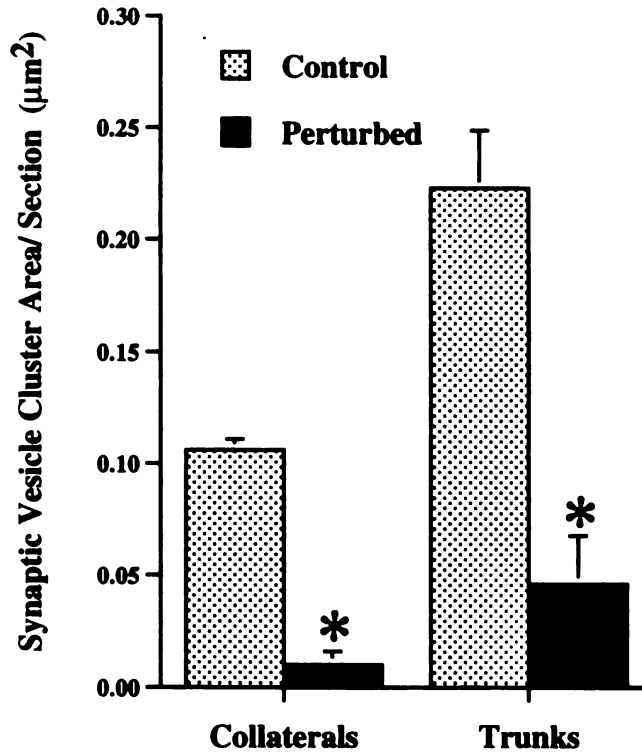


Figure 6. Histogram comparing the amount of synaptic vesicle clusters in control embryos and embryos cultured in the presence of Lan3-2 Fab fragments. Synaptic vesicle clusters were counted in sensory afferent profiles, trunks and branches, that were reconstructed from serial sections cut from CNS ganglia that had been innervated by sensory afferents for 21 hr (MG 14). The difference in the amount of synaptic vesicle clusters was measured by summing the areas with synaptic vesicles in the serial sections of trunks and branches. The trunks and branches in perturbed sensory afferents have six fold less area with synaptic vesicles compared to control embryos. Significantly different than control (*, $P < 0.001$).

Figure 7. Three-dimensional reconstruction of the processes of a sensory afferent in its target region. A sensory afferent was reconstructed, using a Silicon Graphics workstation, from 100 serial sections of a CNS ganglion (MG14 that had been innervated by sensory afferents for 21 hr). To facilitate viewing the three dimensional projections, the reconstructed neuron is divided into five segments separated by sufficient distance to allow viewing of dorsal (front) and ventral (back) processes. The bottom segment represents the proximal aspect of the reconstructed neuron at level 2; the uppermost segment ends close to the midway point between levels 3 and 4. Together, the five segments cover about an 8 μm long posterior to anterior growth of this neuron, assuming a section thickness of 80 nm. The first segment contains the thick trunk of the sensory afferent. The trunk gives rise to its first branches in the upper third of level 2. The other four segments, representing the younger, more distal parts of this neuron consist solely of branches. Only four of the 28 branches of the central arbor extend to the distal edge of the reconstruction.

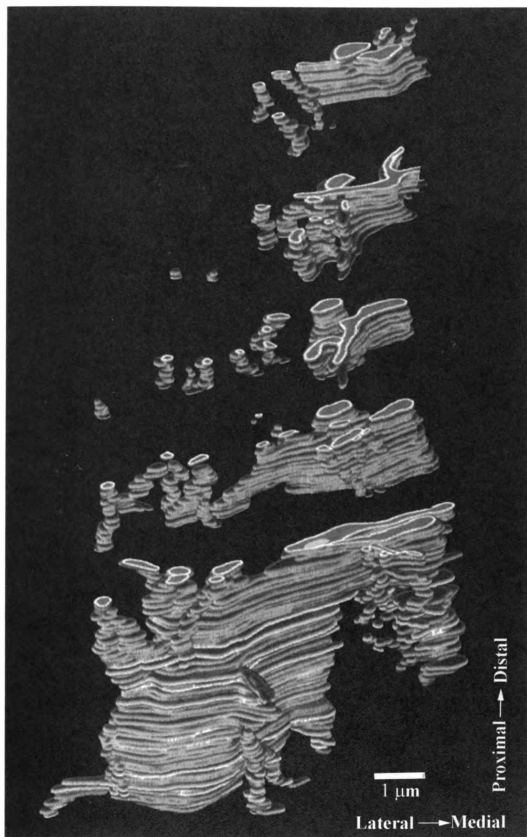
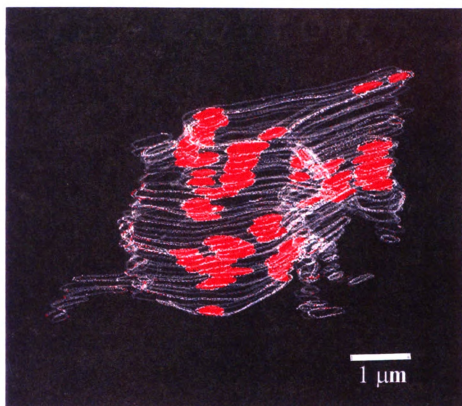


Figure 8. Wire frame reconstruction of a control sensory afferent trunk with synaptic vesicle clusters.

The trunk of the solid reconstruction of the sensory afferent shown in Figure 7 is represented as a wire frame reconstruction to permit the viewing of its synaptic vesicle clusters. The wire frame reconstruction is based on 37 serial sections. The trunk has a total of 14 separate synaptic vesicle clusters, most of which extend over more than one section.

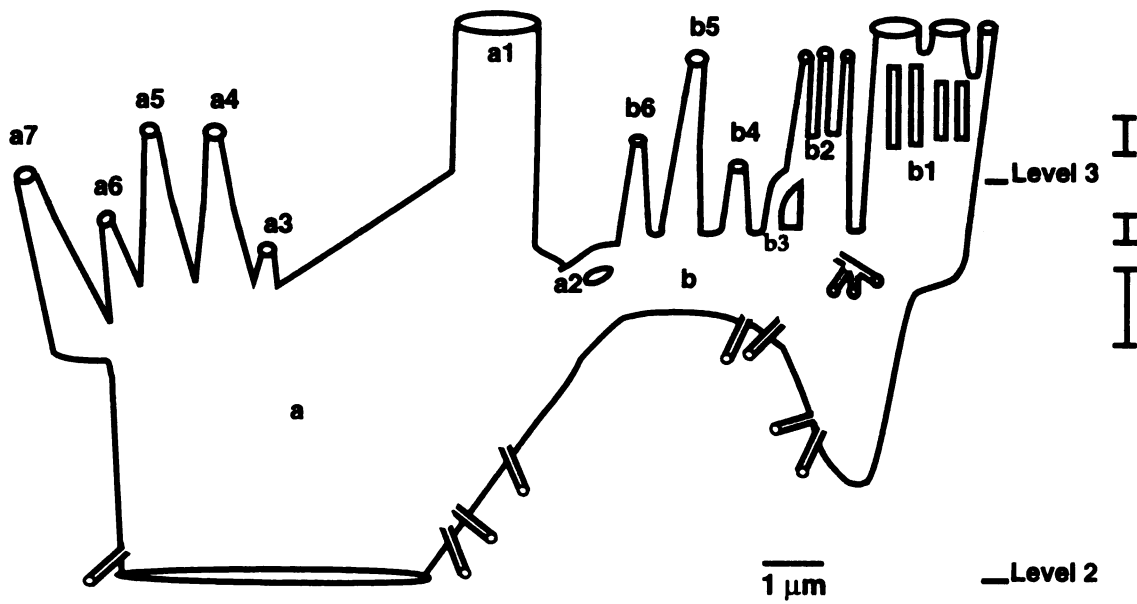


The proximal (posterior) aspect of this neuron (level 2, bottom of picture) consists of a thick trunk (a) with an elliptical cross-sectional area which gives rise to several branches (b, a1- a7), one of which (b) divides again, giving rise to still further branches (b1- b5). Some of the 28 branches that were generated in three distinct branching zones merge again, others die out. At their distal tips, the branches thin out to the diameter of branchlets. Thin branchlets sprout interstitially from the trunk of this neuron. Most of the synaptic vesicle clusters of the trunk extend over several sections. Sensory afferent processes were also analyzed from serial sections (n=3 afferents) in the more recently innervated ganglia MG 16 (not shown). The collateral growth in these recently innervated ganglia, consisting of branches and branchlets (trunks are not yet present), resembled the collateral growth seen at the distal growth region of neurons reconstructed from the older MG 14. Thus, the growth region of sensory afferents is characterized by profuse collateral branching.

Reconstruction of two sensory afferents exposed to Lan3-2 Fab fragments

We also reconstructed sensory afferents from MG 14 that had been exposed to Lan3-2 Fab fragments (n=7). The schematic presentations of two reconstructed sensory afferents (Figure 10 A, B) show different degrees of collateral branching. The sensory afferents with the greatest paucity of branching is illustrated in A. It consists of a trunk that progressively tapers out. The more typical perturbed sensory afferent possesses several branches at its distal growth region. However, these extant branches grow in a fasciculated, rather than in the normal, dispersed manner.

Figure 9. Schematic presentation of a sensory afferent in its target region. The trunk and central arbor of the reconstructed sensory afferent (Figure 6) are presented flattened out into two dimensions to facilitate the analysis of the neuron's collateral growth pattern. Most of the branches are generated at three distinct branching zones (vertical lines). At the first branching zone, the sensory trunk labeled a ends in eight branches, labeled a1 to a7 and b. At the second branching zone, b ends in six branches b1 to b6. In the third branching zone, b1 and b2 give rise to a total of eight further branches (not lettered). Interestingly, there is not only generation of new branches, but also merging of previously generated branches, e.g., b3 merges with b2. Also, the five branches of b1 merge into a common process which then branches again giving rise to three further branches. Most of the branches generated at the three branching zones either merge or thin out into branchlets before terminating. Only four out of the 28 branches in this central arbor extend to the distal edge of the reconstruction. Processes with the dimensions of branchlets also project interstitially off the lateral shaft of the trunk and the thick branches



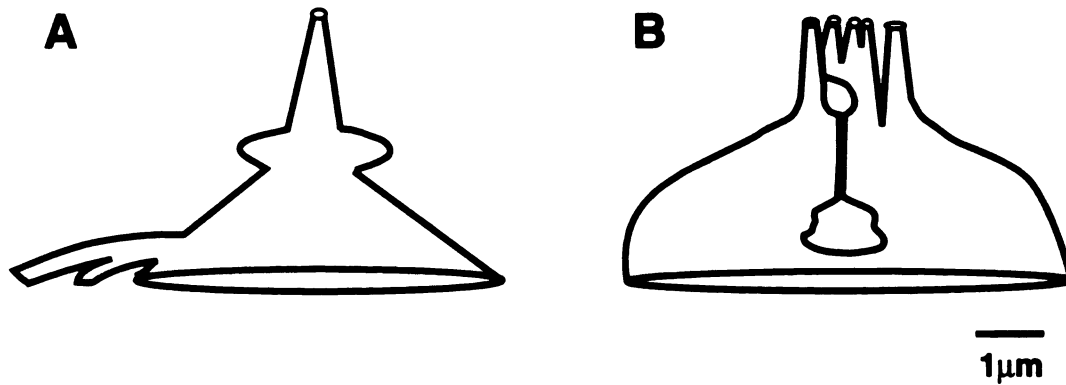


Figure 10. Schematic presentations of perturbed sensory afferents in an embryo cultured in Lan3-2 Fab fragments.

Two sensory afferents are shown that were analyzed from serial sections (level 2) taken from MG 14 of a embryo exposed to Lan3-2 Fab fragments. This experimental embryo is a sibling of the control embryo from which the sensory afferent shown in Figures 7, 8, and 9 had been reconstructed. A) The sensory afferent trunk tapers out into a branch, which in turn thins out into a single branchlet. B) The sensory trunk generates two branches which converge to grow tightly apposed to one another. One of these branches thins out into a branchlet, the other gives rise to four more branchlets. All of the branchlets project in close apposition.

The observed fasciculation of collaterals (Figures 3B and 10) and the reduction in the number of collaterals and size of target areas (Figure 4, Table 1), as a result of antibody perturbation is consistent with the interpretation that the inhibition of mannose-specific recognition leads to a refasciculation of branches, followed by their resorption into a single process.

DISCUSSION

The studies reported here extend previous studies (Song and Zipser, 1995a; Zipser and Cole, 1991; Zipser et al., 1989) on the role of mannose-specific recognition in the formation of central arbors in the CNS of the leech. Here the analysis is taken to the single neuron level using electron microscope. Control embryos show that sensory afferents innervate novel aspects of their future target regions through collateral branching. With ongoing development, collateral branches are replaced by sensory trunks with numerous synaptic vesicle clusters and mitochondria.

Blocking the mannose marker of sensory afferent processes with Lan3-2 Fab fragments led to a rapid and major reorganization of early and later stages of sensory afferent growth. First, the distal growth regions of the sensory afferents lose their collaterals. Second, the developmentally older, more proximal trunk regions of sensory afferents lose their synaptic vesicle clusters. Third, the altered sensory afferent processes grow through the target region at an accelerated rate resembling that of normal sensory afferents elongating through non-target regions. We conclude that mannose-specific recognition plays important roles during different stages of synaptogenesis, including a slowing of process elongation, promotion of collateral branching and synaptic vesicle formation. These results suggest that depriving afferents of their mannose-specific recognition converted afferents that would otherwise be engaged in synaptogenesis back into afferents tracking through non-target regions.

Characteristically, sensory afferents branch into a profusion of collaterals as they enter their target region. Innervation of target regions through collateral branching is a typical process that has been studied in many different brain regions and species (Harris et al.,

1987; Nakamura and O'Leary, 1989; Simon and O'Leary, 1990; Kaethner and Stuermer, 1992; O. Rourke et al., 1994; Bastmeyer and O'Leary, 1996). In the development of leech sensory afferents, collateral growth in the proximal aspect of the target region has been replaced after 14 to 21 hr by a wide sensory trunk. There are at least two possibilities for the transformation from collateral growth to trunk growth that a sensory afferent undergoes with maturation. One possibility is that collaterals are resorbed, giving rise to the widened trunk. Another possibility is that the trunk represents the elongation and widening of the growing sensory afferent axon analogous to the growth of a tree trunk. To distinguish between these two possibilities will require imaging live sensory afferents similar to studies performed on the formation of sensory arbors in the body wall by another type of leech sensory neuron, the pressure cells (Wang and Macagno, 1997).

Blocking the mannose marker with Lan3-2 Fab fragments led to sensory afferents losing their collaterals, both thick branches and fine branchlets, from their growth regions. At the low concentration of perturbing Fab fragments used here, afferents demonstrated on the average a four-fold loss of their collateral growth. Of the serially reconstructed neurons, one showed virtually no branches while the others had a limited number of branches. However, extant branches were fasciculated. This analysis suggests that the process by which central arbors disappear as a result of antibody perturbation involves both fasciculation and resorption of collateral branches. Because extant collaterals in perturbed embryos are clumped together, it appears that refasciculation precedes resorption. It remains to be seen whether this branch fasciculation and resorption due to the inhibition of mannose-specific recognition is part of the normal transformation of collateral growth into sensory trunks.

Compared to sensory afferents in control embryos, sensory afferents in embryos cultured in the presence of Lan3-2 Fab fragments grew more anteriorly through their target region. This suggests that the perturbed afferents grow at an accelerated rate. After a perturbation lasting for three hours, sensory afferents had elongated some 11 μm beyond the distance covered by sensory afferents in control embryos. Normally, sensory afferents elongate through their target region at a rate of 1.6 $\mu\text{m/hr}$. In contrast, the higher rate of growth by perturbed afferents is that observed for normal leech axons elongating through non-target axon tracts (4 $\mu\text{m/hr}$, Braun and Stent, 1989). This result suggests that depriving afferents of their mannose-specific recognition aborts their synaptogenesis and makes them resume a growth rate appropriate for tracking through axonal tracts. Similar differences in the rate of growth of axons through fibertract and target regions were observed in other systems (Harris et al., 1987; Halloran and Kalil, 1994).

Mannose-specific recognition does not appear to affect pathfinding or navigation per se because sensory afferents exposed to Lan3-2 Fab fragments continue to elongate through their target region without deviation in their path. Because sensory afferents, deprived of their mannose-specific recognition, grow as fasciculated bundles, the bundling presumably is mediated by other molecular mechanisms. One possibility is that axonal bundling involves the RGD binding motif of leech tractin expressed by these neurons (Huang et al., 1997). Recently, genetic studies performed on nematodes provided evidence that integrins (which bind to RGD) mediate axonal fasciculation rather than axonal extension (Baum and Garriga, 1997).

The mannose marker, rather than instructing afferents where to grow, might instead permit them to branch in their target region similar to the action of the polysialic acid

epitope (PSA) of NCAM in the defasciculation and branching of motor and corticospinal axons (Landmesser et al., 1990; Daston et al., 1996). While the effect of PSA on the branching of motor axons is attributed to its negative charge (Rutishauser et al., 1988), the branching mediated by the mannose marker presumably depends on its interaction with an as yet unidentified mannose-binding protein specific to the neuropil of CNS ganglia.

Blocking the mannose marker with Lan3-2 Fab fragments also affects the developmentally older sensory trunks. Sensory trunks lose their synaptic vesicles during a brief three-hour incubation with Lan3-2 Fab fragments. The three-hour time period over which the synaptic vesicle clusters are lost parallels the time period over which such synaptic vesicles clusters are formed in another invertebrate system (Yoshihara et al., 1997). The loss of synaptic vesicle clusters in leech sensory trunks is more severe (six fold) than the loss of collaterals (three to four fold) at the growth region of the same neuron. This rapid and severe loss of synaptic vesicle clusters as a result of antibody perturbation is consistent with the idea that the mannose marker is directly involved in mediating their formation. At the early stage of synaptic vesicle cluster formation studied here, there are no other discernible pre and postsynaptic specializations. Three and a half days later, in 14 day old embryos, other synaptic specializations such as the thickening of the postsynaptic membrane have taken place (McGlade et al., 1990).

One possible explanation for the action of the mannose marker during different stages of sensory afferent synaptogenesis is its developmentally regulated expression on different proteins. As sensory afferents newly innervate the midbody ganglia, the mannose marker is only located on N-linked carbohydrate chains of a 130 kD protein (McGlade-McCulloh et al., 1990) with the solubility properties of a peripheral membrane protein (Bajt et al.,

1990); this protein may be LeechCAM or Tractin or both (Huang et al., 1997). In contrast, with ongoing development, the mannose marker appears on N-linked carbohydrate chains of 103 and 95 kD proteins with solubility characteristics of integral proteins. It is tempting to speculate that the early expression of the mannose marker on peripheral proteins mediates collateral branching, while the later expression of the mannose marker on integral membrane proteins mediates synaptic vesicle formation in sensory trunks.

Another molecular transformation of the sensory afferents is their developmentally regulated expression of galactose-containing markers restricted to 130 kD proteins with solubility characteristics of peripheral membrane proteins. These galactose-containing markers divide sensory afferents into subsets that correlate with different sensory modalities (Zipser et al., 1994; Song and Zipser, 1995b). Thus, the leech embryo represents a suitable system for studying the coordinated action of different carbohydrate markers in synaptogenesis in CNS target regions.

CHAPTER 2. IDENTIFICATION OF THE SENSORY MODALITY OF THE SUBSET
OF SENSORY AFFERENTS WHICH EXPRESSES A HIGH
CONCENTRATION OF LEECH GALECTIN AND IDENTIFICATION
OF ITS POTENTIAL POSTSYNAPTIC PARTNERS.

In this chapter, we characterize a subset of leech sensory afferents, the photoreceptors, in terms of their molecular composition, anatomical distribution and candidate postsynaptic partners. For reagents, we used an antiserum generated against purified LL35, a 35 kD leech lactose-binding protein (galectin); mAb Lan3-2; and dye injections. Photoreceptors differ from other types of sensory afferents by their abundant expression of galectin. However, photoreceptors share in common with other sensory modalities the mannose-containing epitope recognized by mAb Lan3-2. Photoreceptors from a given segment project their axons directly into the CNS ganglion innervating the same segment. They assemble in a target region, the optic neuropil, which is separate from the target regions of other sensory modalities. They also extend their axons as an optic tract into the connective to innervate optic neuropils of other CNS ganglia, thereby providing extensive intersegmental innervation for the 32 CNS ganglia comprising the leech nerve cord. Because of its intimate contact with the optic neuropil, a central neuron, the AP (anterior pagoda) effector cell, is a strong candidate second order visual neuron. In confocal images, the AP cell projects its primary axon for about 100 μm alongside the optic neuropil. In electron micrographs, spines emanating from the axon of the AP cell make contact with vesicle laden nerve terminals of photoreceptors. Leech photoreceptors

and their second order visual neurons represent a simple visual system for studying the mechanisms of axonal targeting.

INTRODUCTION

The leech is a useful model system for the investigation of the developmental function of carbohydrate markers on neuronal surfaces. We previously demonstrated that surface carbohydrates mediate sequential steps of axonal targeting at the level of the synaptic neuropil (Song and Zipser, 1995a, b; Zipser, 1995). Some of these surface carbohydrates serve as specific markers for the full set and for different subsets of sensory afferents. Several lines of evidence support the hypothesis that these carbohydrate markers are related to sensory modality of afferent subsets, e.g. encode mechano-, chemo- and/or heatdetector function (Zipser, 1994). In other invertebrate and vertebrate organisms, carbohydrate markers also delineate different sets and subsets of neurons (Dodd and Jessell, 1986; Jessell et al., 1990) and perhaps play similar developmental roles.

In this chapter, we are concerned with the potential role of carbohydrate binding proteins in axonal targeting. Classically, carbohydrate recognition events involve the interaction of carbohydrates with lectins or enzymes, two types of carbohydrate binding proteins (Sharon and Lis, 1989); though recently there have been some reports of carbohydrates interacting among themselves, that is, homophilically (Misevic and Burger, 1993; Dammer et al., 1995). In contrast to the abundant information on the distributions of different carbohydrate moieties on neuronal sets and subsets or at synapses (as reviewed in Sanes and Cheney, 1982; Jessell et al., 1990), there are fewer studies about the distributions and functions of lectins in the nervous system (Hynes, 1990; Mahanthappa et al., 1994; Cole and Zipser, 1994b).

To lay the groundwork for investigating the role of lectins in the nervous system, we have identified the function of a subset of neurons that expresses galactose-binding lectin or galectin (Cole and Zipser, 1994a, b). We provide several lines of evidence that these galectin positive neurons are sensory afferents specialized for photoreception. We also identify the AP effector cell as a likely postsynaptic partner for these sensory afferent neurons (Tai et al., 1996). Using double-labeling techniques, we demonstrate that photoreceptor axons extensively colocalize with processes of the AP cell. Ultrastructural analysis confirmed that the nerve terminals of photoreceptors make direct contact with AP cell processes. The precise nature of these contacts, both physiological and structural, remains to be determined.

MATERIALS AND METHODS

All experiments were performed on individuals of the leech species *Hirudo medicinalis*, which were bred at room temperature (23°C) in diluted artificial sea water and fed with fresh bovine blood once a month. After isolation for 2 months at 15°C, adult leeches were brought together in pairs for mating for about 1 month at room temperature. The gravid leeches were then placed in plastic boxes containing moist sphagnum moss. Boxes were checked daily for cocoons. Once found (day 0), cocoons, each containing 12-18 sibling embryos of the same age, were transferred to an incubator at 20°C. To obtain juvenile leeches, cocoons were kept in the incubator (20°C) for about a month until hatching.

Antibodies

The antibodies used in this study were generated by our laboratory. Lan3-2 is a mAb that binds to the full set of peripheral sensory afferent neurons (Zipser and McKay, 1981; Zipser et al., 1994). Conjugation of HRP and rhodamine to mAb Lan3-2 is performed according to the methods of Avrameas and Ternynck (1971) and Harlow and Lane (1988), respectively. Directly labeled Lan3-2 is used for staining the surface of live sensory afferent neurons (see below). The antiserum to galectin was generated by immunizing rabbits with purified 35 kD leech galectin. In addition, it was affinity purified against 35 kD galectin (Cole and Zipser, 1994 a, b).

Immunostaining of photoreceptors with galectin antiserum

To immunostain photoreceptors in the embryonic head, it was necessary to digest the cuticle with papain. Live 13 to 14 day-old embryos were treated for 1 hr with 6 μ l of mercuripapain (Worthington Biochemical Corp., NJ) in 100 μ l phosphate buffered saline (PBS), pH 7.4, containing 5 mM EGTA (Sigma) and fresh cysteine (1.6 mg/10ml, Sigma). Mercuripapain was preincubated in the EGTA containing buffer for 0.5 hr prior to digestion so that papain would be activated by the removal of mercury through EGTA. Embryos were either fixed with 4 % paraformaldehyde (Sigma) in 0.1 M PBS (pH 7.4) or washed with culture medium L-15 and subsequently treated with 5% fetal calf serum (Gibco) in L-15 to quench papain. For fixed embryos, subsequent immunostaining was performed using PBS containing 2% Triton X-100 (TX-100, Sigma) and 3% bovine serum albumin (BSA, Sigma); for live embryos, immunostaining was performed using L-15 medium. Embryos were first incubated overnight in the presence of galectin antiserum (1/1, 000 to 1/5, 000), then rinsed and treated for 2 hr with biotinylated goat-anti rabbit Fab fragments (diluted 1/800; DAKO, Carpinteria, CA) and finally treated for 1 hr with avidin-FITC (1/1,000; Vector, Burlingame, CA). Fixed embryonic heads were rinsed with PBS (pH 7.4), live embryonic heads were rinsed with L-15. Antibody incubations were carried out on a shaker (200 rpm) at room temperature. The tissues were then embedded in 70% glycerol/30% glycine to which saturating levels of p-phenylenediamine (Sigma) had been added to prevent the bleaching of fluorescence. The tissue was analyzed on a Laser Scanning Confocal microscope (see below).

To immunostain photoreceptor axons in the nerve cord, embryos were fixed without papain treatment. Antibodies were visualized with HRP-conjugated avidin (diluted

1/800; Vector), followed by the the DAB reaction. The tissue was embedded in Permount and viewed under the light microscope.

Double-labeling of photoreceptors in embryos

Leech embryos (25 to 30 day-old) were anesthetized with 0.05% chlorobutanol and then pinned against Sylgard (184 silicone, Dow Corning Co., Midland, MI) - coated culture dishes (35 x 10 mm) (Corning Glass Works, Corning, NY). The eyes of embryos were injected with diO [3,3'-dioctadecyloxacarbocyanine perchlorate; diO-C18-(3)] (Molecular Probes, Eugene, OR), from a microelectrode filled with 1% diO (w/v in ethanol: DMSO (1:1)). After injection, the embryos were removed from the Sylgard culture dish and kept in a 20°C incubator for two weeks. After two weeks, head ganglia and anterior ganglia were dissected out and stained for the full set of sensory afferents using overnight incubation with the rhodamine-conjugated mAb Lan3-2 in culture medium L-15. Antibody incubations were carried out on a shaker (200 rpm) at room temperature. The ganglia were first rinsed with PBS, pH 7.4 and then embedded in glycerol as above. The fluorescently double-labeled ganglia were analyzed on a Laser Scanning Confocal microscope (see below).

Double-labeling of live pre- and postsynaptic neurons in juvenile ganglia

Juvenile leeches were anesthetized with 5-8 % ethanol. Midbody ganglia were dissected out from the blood sinus and pinned against Sylgard-coated dishes containing leech Ringer's solution. The outer capsules of the ganglia were removed using fine forceps. The live ganglia were cultured overnight in culture medium L-15 in the presence

of rhodamine-conjugated mAb Lan3-2 to stain the full set of sensory afferents. Five different types of CNS neurons, AP cells, N (nociceptive) cells, T (touch) cells, Retzius cells and AE cells, were pressure injected with Lucifer yellow (3-10 % w/v 0.1 M LiCl₂) (Molecular Probes). After the dye had diffused through the cell for 15 min, the tissue was fixed for 1/2 hr in 4% paraformaldehyde in 0.1M PBS (pH 7.4), and then mounted in glycerol as above. The specimens were analyzed on the confocal microscope.

Ultrastructural analysis of connections in juvenile ganglia

Juvenile leech ganglia were prepared as described previously. Live ganglia were kept in culture medium overnight in the presence of HRP-conjugated mAb Lan 3-2. The leech ganglia were then rinsed 3 times with tissue culture medium and pinned against Sylgard-coated dishes also containing tissue culture medium. One AP cell per midbody ganglion was pressure injected with HRP (20 mg/ml, Type IV; Sigma). After the HRP injection, the ganglia were cultured for another hour to allow HRP to diffuse from the cell bodies down into the axons and neurites. Afterwards, the ganglia were fixed for 1/2 hr in 2% glutaraldehyde in 0.1M PBS (pH 7.4). After fixation, the tissue was rinsed with 0.1M PBS for 15 min and then preincubated for 10 min in a fresh solution of 0.5 mg/ml DAB. The chromogen reaction was started with a few drops of 0.3% H₂O₂ and terminated by rinsing three times with PBS. The tissue was post-fixed with 1% osmium tetroxide (Ted Pella, Inc., Redding, CA) for 2 hr, dehydrated with serial changes of alcohol and then transferred into propylene oxide to be finally embedded in English araldite resin. Ultrathin sections were cut on an LKB Ultratome V, collected on copper slot grids and

stained with 10% uranyl acetate and Reynold's lead citrate section stain. Grids were examined with a Phillips CM10 at 100 kV.

Data analysis of immunocytochemical stained tissue by confocal microscopy

The fluorescently stained tissue was examined with the Odyssey, a Real Time Laser Scanning confocal microscope (Noran Instrument Inc., Madison, WI). Serial sections were captured with 10, 25 (Zeiss), 60 or 100 (Nikon) x oil immersion objectives. The laser excitation and primary barrier filters for fluorescein and rhodamine were 488, 515 nm and 529, 550 nm respectively. DiO anterogradely labeled photoreceptors and Lucifer yellow-labeled neurons were examined with fluorescein isothiocyanate (FITC) optics. The projections of photoreceptors in head ganglia and anterior ganglia were captured in 10 serial optical sections taken at 1 μm steps through the synaptic neuropil. To reconstruct three-dimensional images or to analyze the data, the optical sections were processed with Image-1 program (Universal Image Co., West Chester, PA). The double-labeled juvenile ganglia were optically sectioned at 2 μm steps (10x objective) or 1 μm steps (60x oil immersion objectives) and the sections were used to build three dimensional reconstruction from which RGB images were formed.

RESULTS

Abundant expression of galectin is a marker for the leech photoreceptor neurons

Halfway through embryonic development (14 day-old), a few cell bodies in the large sensilla of the midbody region contain lactose-binding protein or galectin. These sensory neurons and their axons which project centrally can be stained with an antiserum which was generated and affinity purified against soluble 35 kD leech galectin (LL35) (Cole and Zipser, 1994a, b). Their small number/sensillum and their lack of an apical process has suggested that these cell bodies may be the sensillar photoreceptors (Phillips and Friesen, 1982). To determine whether galectin is a marker for all photoreceptors, we examined the embryonic eyes on the head of the leech for galectin expressing cell bodies and axons.

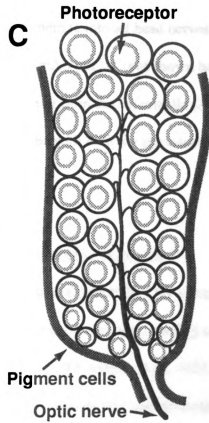
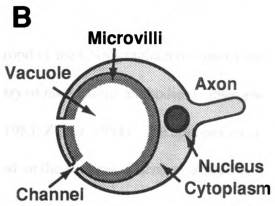
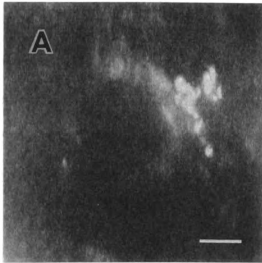
Photoreceptors in the eyes were immunofluorescently stained by incubating 13 to 14 day-old embryos (4 fixed embryos and 6 live embryos) with the antiserum to galectin (Figure 11). At this developmental stage, the five pairs of eyes are easily discerned on the anterior segments of the leech head by their densely clustered, large, round photoreceptor cell bodies even though the tissue surrounding each eye has not yet acquired pigment. Using confocal microscopy, we sectioned through the epithelial cell layer into eyes 1 and 2. In these optical sections we were able to resolve weakly immunostained cell bodies of photoreceptors (Figure 11A, from a fixed embryo). The thin cytoplasmic rim of the photoreceptor cell body (2 μm wide) was galectin positive while the large vacuole inside the cell body was unstained (Figures. 11A and B). Treating live embryos with the galectin antibody also led to photoreceptor staining (not shown) suggesting that galectin is present not only in the cytoplasm but also on the cell surface. In all embryos, the axons

Figure 11. The cell body and axon of a photoreceptor in leech eye are galectin immunoreactive.

A) A 13 day-old embryo was stained with antiserum to leech lactose-binding protein or galectin (Cole and Zipser, 1994a; Cole and Zipser, 1994b). Eye 2 was optically sectioned. The confocal image, representing the sum of 8 optical section (60 x) shows the cell body of a photoreceptor exhibiting galectin immunoreactivity. Only the thin cytoplasmic rim of the cell body is stained, while its large, central vacuole is unstained. The weakly stained cell body projects a more brightly stained axon. The weak staining arises from the wholemount preparation presenting barriers to antibody penetration across cuticle, epidermis and borders of the eyecup. Calibration bar = 10 μm

B) and C) Diagrammatically illustrate the histology of the leech eye (as adopted from Hansen, 1962, Röhlich and Török, 1964). B) The cell body of the photoreceptor surrounds an extracellular compartment, the "vacuole", which communicates with intercellular spaces through narrow channels (Lasansky and Fuortes, 1969). The translucent proteinaceous material of the vacuole ("glasskörper") is thought to serve as a lens for the photoreceptor (Röhlich and Török, 1964). The microvillar membrane (Walz, 1979) of the vacuole changes its conduction in response to light (Fioravanti and Fuortes, 1972; Lasansky and Fuortes, 1969; Peterson, 1983), leading to a rise in Ca^{2+} inside the cytoplasm (Wulf, 1982). The cytoplasm is packed with mitochondria, multivesicular bodies, endoplasmic reticulum, and many small vesicles (500 to 600 Å). In the drawing in B, the lightly shaded region represent the galectin immunoreactive cytoplasm in A. Other features of the photoreceptor such as the vacuole, the microvilli and the channels are not stained with galectin antiserum.

C) The cell bodies of photoreceptors are collected into eyecups. The top of an eyecup is covered with a single layer of transparent epithelial cells while its sides are delimited by a layer of pigment cells. At embryonic day 13, the pigment cells are still colorless, but they are yellow by embryonic day 15, green by embryonic day 18, and black in the adult. Inside the eyecup (Hansen, 1962), the round cell bodies of these photoreceptors are arranged in 6 to 10 layers, in the top layers they are between 30-45 μm in diameter, in the middle and bottom layers, they are 20-30, and 12-20 μm in diameter, respectively. In addition, there are what may be an additional class of photoreceptors, the "Sonderzellen", at the bottom of the eyecup. The cell bodies of photoreceptors are associated with fine processes which according to Röhlich and Török (1964), resemble those of glial cells (but see, Lasansky and Fuortes, 1969). Photoreceptor cell bodies are separated from one another by connective tissue containing fine muscle fibers (not drawn). Photoreceptors project their axons medially into the center of the eyecup where they fasciculate into a bundle which projects down along the midline of the eyecup to exit through a hole at bottom of the eyecup as an optic nerve.



of these photoreceptors were significantly more strongly stained than the cell bodies. Immuno-stained axons were observed to emanate from the eyes, but not from any other sensory organs in the head such as the lip sensilla which contain chemoreceptors (Elliott, 1987). To demonstrate that antibody was able to penetrate into all head nerves under these conditions, sibling embryos were treated with mAb Laz1-1 (not shown here) which readily stained the axons of chemoreceptors emanating from the lip sensilla (Zipser et al., 1994). Thus, galectin is a neuronal marker associated with both the photoreceptors in the eye and those in the midbody sensilla.

Target region of photoreceptors in the synaptic neuropil of CNS ganglia

The projections of sensory afferents through peripheral nerves into the synaptic neuropil of the CNS ganglia have been studied with immunostaining, making use of a library of monoclonal antibodies (Zipser and McKay, 1981; Flaster et al., 1983; Hogg et al., 1983; Zipser, 1994). The epitopes recognized by these monoclonal antibodies are found on the surfaces of sensory afferents, where they are located on the N-linked carbohydrate chains of the 130 kD sensory afferent proteins (Bajt et al., 1990). The epitope recognized by mAb Lan3-2 serves as a carbohydrate marker for the full set of sensory afferents, while epitopes recognized by other mAbs serve as carbohydrate markers for 4 disjoint subsets of these same sensory afferents (Johansen et al., 1992; Zipser, 1994). Three sensory afferent subsets, identifiable by their different carbohydrate markers, project into a lateral cluster of four target regions. Because several lines of evidence suggest that these carbohydrate markers are related to sensory modality, mechano-, chemo- and possible heat detection, we consider the lateral cluster of four

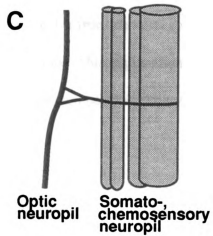
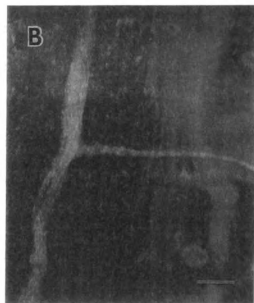
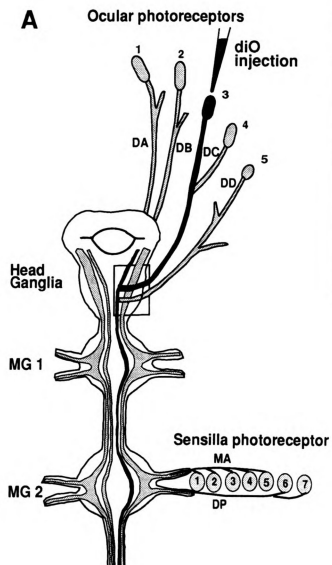
target regions to represent the somato-, chemosensory neuropils (Figure 12C) (Peinado et al., 1990; Zipser, 1994). The sensory modality which projects into the fifth target region near the midline is studied here. Of these five target regions, only the one nearest the midline (Figure 12) is immunoreactive for galectin [see Figure 15A and previous studies (Cole and Zipser, 1994b)]. To confirm that this target region is an optic neuropil, we injected the eyes of live embryos with the lipophilic dye diO (green fluorescence; Figure 12B). To visualize all sensory afferent target regions, the same live embryos were also exposed to rhodamine conjugated mAb Lan3-2 (red fluorescence; Figure 12B). This mAb binds to the surfaces of all sensory afferents and therefore stains both the optic neuropil, which is closer to the midline, and the other four target regions comprising the somato-, chemosensory neuropils, which are closer to the lateral ganglionic margin.

After injecting each of the leech eyes with diO (9 embryos, injection of 1 eye; 6 embryos, injection of 2 eyes), fluorescent photoreceptor axons were observed to project into the CNS, via their respective peripheral nerves (DA, DB, DC, DD, Figure 13A). The confocal image (Figure 12B) was taken from the right neuropil of a head ganglion of an embryo whose ipsilateral third eye had been injected with diO. After entering the head ganglia (Figures. 12B and C), the diO labeled photoreceptor axons do not enter the somato-, chemosensory target region, but instead project medially for another 70 to 100 μm as a tightly bundled axon tract which then bifurcates upon entering the sensory afferent target nearest to the ganglionic midline. This finding indicates that the sensory afferent target region closest to ganglionic midline is the optic neuropil. Photoreceptor axons project ipsilaterally into an optic neuropil, they do not cross the midline.

Figure 12. DiO injection of photodetectors.

A. Five leech eyes, arranged as pairs on the anterior segments of the head of the leech, project their axons via the appropriate head nerves (DA, DB, DC, and DD, as adopted from Kretz et al. (1976)) into the supra-, and subesophageal head ganglia. In addition, there can be about 2 to 3 sensillar photoreceptors in most if not all of the 7 large sensilla on the central annuli of the body wall segments which project their axons via peripheral nerves into the 21 segmental ganglia of the midbody region (MG1, MG2, etc.). Sensory afferent target regions extend throughout the CNS (hatched areas). The optic neuropil is closest to the ganglionic midline; the somato-, chemosensory neuropils (consisting of four closely apposed subregions which are not separately indicated here) are closest to the lateral ganglionic margins. The boxed area in the subesophageal ganglia is shown enlarged as a confocal image (25 x) in B and as a diagram in C. Calibration bar=25 μ m.

B) and C) The central projections of photoreceptors were traced by injecting eye 3 with diO (yellow/green fluorescence). Additionally, in the same live embryo, all sensory neuropils occupied by the peripheral sensory afferents were identified through staining with rhodamine-conjugated mAb Lan3-2 (red fluorescence). Photoreceptor axons (yellow/green in B and black in C) project medially as a tightly fasciculated optic nerve past the cluster of 4 somato-, chemosensory neuropils, shown as unresolved red band in B and drawn as four separate tract (shaded gray) in C, based on previous studies (Zipser et al., 1994). In this unfixed preparation, the slow deterioration of ganglionic neurons also produces red autofluorescence as background staining. Close to the midline, the bundle of photoreceptor axons bifurcates and enters the 5th sensory target region, which we now consider to be the optic neuropil. (Peterson, 1984) had observed dye-coupling into photoreceptor axons, in what we have now demonstrated to be the optic neuropil, after injecting Lucifer yellow into a second order visual cell, the LV cell.



To test for intersegmental projections of photoreceptor axons, we also confocally sectioned the more anterior CNS ganglia of the midbody region. In all embryos with eyes injected with diO, fluorescent photoreceptor axons were detected in the optic neuropil of midbody ganglion 1 (MG1). In 9 embryos, fluorescent axons could be followed posteriorly as far as midbody ganglion 4. Because of the problem that diO may diffuse transcellularly with extended incubation times, we did not allow longer times for diO diffusion which may have stained photoreceptor axons in more posterior CNS ganglia.

In addition to the strong diO staining of axons in the optic neuropil, there was also some, much weaker staining of the other four sensory afferent target regions specialized for somato-, and chemosensory projections. This weak labeling of these neuropils was seen in 40% of the injected embryos in the head ganglia and in 55% of the injected embryos in midbody ganglion 1. This weak labeling could be due to a small percentage of the photoreceptors sending collaterals to the other target regions. Alternatively, the weak labeling could be due to the diffusion of the lipophilic dye from photoreceptor axons into the axons of other types of sensory afferent neurons. This explanation would be likely if different sensory neurons run closely bundled through peripheral nerves.

Candidate postsynaptic neurons for sensory afferents.

We also used a double-labeling method to search for candidate synaptic partners for sensory afferent neurons. Different types of central neurons were injected with Lucifer yellow: effector cells, such as the AP, Retzius and AE cells, and central sensory neurons, such as the P cells and N cells (Muller et al., 1981). In addition, sensory afferent neurons were immunostained with rhodamine-conjugated mAb Lan3-2. Using confocal

microscopy, the synaptic neuropils of midbody ganglia were scanned for the processes of central neurons (yellow/green) that projected into the sensory afferent target regions (red).

Of the five types of neurons tested, the AP cell contacts the optic neuropil over the longest distance via its primary axon. As seen in the confocal image and diagram (Figures 13A and B), the cell body of the AP cell is located in the cortex of the CNS ganglion. It projects a large primary axon medially across the synaptic neuropil and then bifurcates, giving rise to a branch into both the contralateral anterior and posterior roots on its way to its peripheral targets. Sensory afferent processes (all modalities, red), enter the ganglion via the anterior and posterior roots and project into the somato-, chemosensory and optic neuropils. Additionally, sensory afferents project between the segmental ganglia via the connective.

The AP cell processes extensively colocalize with photoreceptor axons in the contralateral optic neuropil (Figure 13C). The large primary axon of the AP cell (green) projects alongside the optic neuropil over a distance of 93 μm . Furthermore, AP cell processes also colocalize with sensory afferents in the junctional area between the somato-, chemosensory neuropils and the roots, a region where it could potentially contact all sensory afferent modalities (Figure 13D).

The other two effector cells tested, the AE and Retzius cells, do not project primary axons close to the optic neuropil but only thin, secondary processes. The two central neurons tested, the P and N cell only demonstrate a slight degree of colocalization of a few branches with the optic neuropil (Figure 14).

Figure 13. Colocalization of AP cell projection with sensory afferents.

A) A low power confocal micrograph (10 x; 13 optical sections taken at 2 μm steps) illustrates a leech ganglion double-labeled for all sensory afferents with mAb Lan3-2 (red) and the Lucifer yellow injected left AP cell (yellow-green). Crossing the ipsilateral side of the ganglion, the primary AP cell axon does not run in close proximity to the somato-, chemosensory or optic neuropils. Instead, it contacts the contralateral optic neuropil; the site of contact is bleached because it was first studied at higher power as illustrated in C.

The Calibration bar shown in D applies to all confocal images, in A = 60 μm , in C and D = 10 μm . Anterior is up.

B) Diagrammatic representation of a leech CNS ganglion in the midbody region. Sensory afferents enter the CNS ganglia via three separate axon bundles from the anterior and posterior roots. The different sensory modalities then project in a stereotypic pattern, exhibiting convergence and divergence, into the 4 chemo-, mechanosensory neuropils (Zipser, et al., 1994) and the more medially situated optic neuropil. The small axon bundles projecting from the root into the optic neuropil are not shown. After having innervated the CNS ganglion of the segment of their origin, sensory afferents also project intersegmentally via the connective to innervate sensory afferent neuropils of other CNS ganglia. A central neuron, the AP cell is located in the cortex of each ganglion and projects its large primary axon contralaterally. The primary axon bifurcates after it passes the contralateral optic neuropil and its two branches exit the contralateral anterior and posterior roots to innervate peripheral targets.

C) High power confocal micrograph (60x; 8 optical sections taken at 1 μm steps) illustrates the region of close apposition - over a 93 μm stretch - of the large AP cell axon (green) with the optic neuropil (red). At the top of the confocal image (anterior), the AP cell axon projects alongside the optic neuropil; at the bottom of the image (posterior), the AP cell axon crosses the optic neuropil.

D) A high power confocal micrograph (60x; 6 optical sections taken at 1 μm steps) illustrates the colocalization of varicose processes of the AP cell (yellow green) with sensory afferents (red) at the junction of the neuropil with the anterior root. As the Image-1 software sums the optical sections taken with RITC and FITC optics, it assigns yellow to pixels with the same x/y (anterior/posterior) coordinates that are stained with both types of illumination, even though they may be far apart in the z (ventrodorsal) dimension. In the summed image in A, the green stained AP cell axon turns yellow as it passes by the ipsilateral sensory afferent target region at considerable distance in the z dimension. In contrast, in C and D, the yellow areas represent areas of true colocalization because they are seen in the same optical section captured first with RITC and then with FITC optics.

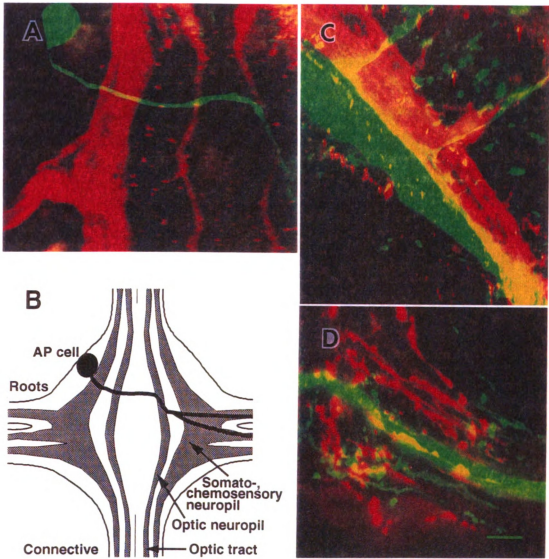
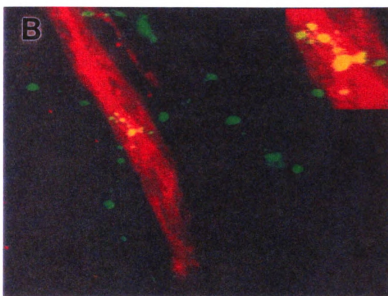
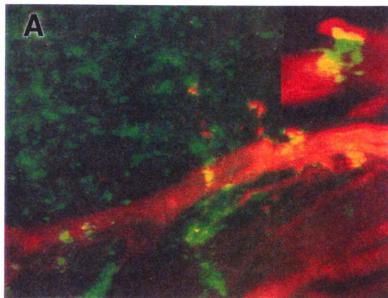


Figure 14. Colocalization of Retzius cell and N cell with sensory afferents.

A) Colocalization of Retzius cell neurites and varicosities with the sensory midline tract. The Retzius cell neurites and varicosities overlapping with the red-stained sensory afferent tract are labeled yellow whereas the nonoverlapping Retzius cell neurites are labeled green. Fourteen optical sections were taken at 1 micron steps with rhodamine and fluorescein optics and summed. The insert showing a Retzius varicosity superimposed on the midline tract is from a single focal plane, magnified 4 times.

B) Colocalization of the N cell with sensory afferents in the sensory midline tract. N cell varicosities overlapping with the red-stained midline tract appear yellow. The N cell varicosities outside the sensory afferent tracts appear green. Five optical sections were taken at 1 micron steps and summed. The insert showing N cell varicosities apposed to the midline tract are from a single focal plane, magnified 4 times.



Sensory afferents are presynaptic to the AP cell.

To investigate whether the AP cell is indeed a candidate postsynaptic partner of photoreceptors and other types of sensory afferent neurons, we modified the double-labeling method used for our confocal analysis. In the same live ganglion, sensory afferent neurons were identified with HRP-conjugated Lan3-2, while the cell body of an AP cell was injected with dissolved HRP. In electron micrographs, sensory afferents are identified by DAB reaction product on their surface membrane while the processes of the AP cells are identified by DAB in their cytoplasm. We identify Lan3-2 labeled axons as belonging to optic neuropil photoreceptors on the basis of their proximity to the ganglionic midline and their distance from the somato-, chemosensory neuropils into which the other sensory modalities project. This relationship was described fully at the confocal level (Zipser, 1994).

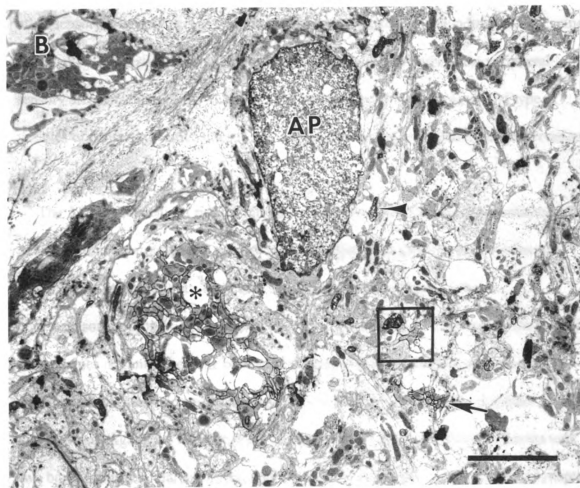
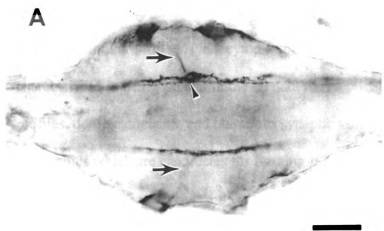
As seen in Figures 15B and 17, the primary axon of the AP cell runs at a short distance (about 5 μm) from the major bundle of photoreceptor axons in the optic neuropil. This bundle consists of a coherent group of 60 to 80 axonal profiles, all of which appear to be Lan3-2 immunoreactive on their cell surface. Nearby, smaller groups of surface-labeled neurites (1-10) are often seen running parallel to the major bundle but separated from it by unstained axonal profiles and glia. The finding that individual or small groups of processes separate from the main bundle is consistent with the "loose" appearance of the photoreceptor projections often seen in the confocal light micrograph (e. g. Figure 15A, arrow head).

The AP axon gives rise to thin spinelike processes that extend several microns toward the optic neuropil. These spines come into direct contact with small bundles of Lan3-2

Figure 15. Optic neuropil and AP cell processes.

A) A segmental midganglion was treated with affinity purified antiserum to leech galectin 35 (LL35). The only sensory afferent target regions that are galectin positive are the left or right optic neuropils near the ganglionic midline. Anterior is left. Sensillar photoreceptor axons project as thin axon bundles from right and left anterior roots (arrow) into their respective ipsilateral optic neuropil. Note the "loose" appearance of the photoreceptor projections (arrow head). The stain at the edges of the ganglion represents epithelial cells from the capsule covering ganglia and roots. While galectin is a specific neuronal marker for photoreceptors, it is also expressed by epithelial cells (Cole and Zipser, 1994b). Calibration bar=20 μ m

B) TEM cross section through the left side of a juvenile leech CNS ganglion in the midbody region, approximately 1/3 of the way between the anterior entry point of the interganglionic connectives and the anterior nerve root. The thick axon of the AP cell (AP) and several (4-5) of its spine-like projections (arrow head) have been filled with HRP, and visualized with the DAB reaction product. The main bundle of photoreceptor axons forming the optic neuropil (*) has been identified with HRP conjugated mAb Lan3-2, which recognizes a surface epitope on all sensory afferents. On the lower right is a small cluster of labeled axons (arrow), which we also presume to be a part of the optic neuropil. The region in the box is shown at higher magnification in Figure 16. Calibration bar = 5 μ m



labeled axons where they have separated from the main group of photoreceptor axons by a few microns (Figures. 15B, 16, 17). Direct contacts of photoreceptor neurites with the spinelike processes emanating from the AP axon took two forms: In the first, the neurites had small circular profiles, clear cytoplasm, microtubules, and few vesicles. These we characterized as being axons. In the second, the labelled neurites had irregular, larger profiles, dense cytoplasm, and numerous synaptic vesicles. We characterized these as varicosities which are candidates for forming functional synaptic contact with the AP spine projections. In no case did we find direct contact between surface labeled photoreceptor neurites with the main AP axon. In the neuropil of the optic tract (and the other sensory afferent tracts as well) not all of the varicosities surrounding the AP "spine" are labelled, suggesting that input may also arise from sources other than peripheral sensory afferents identified by Lan3-2. The appearance of the cytoplasm and type of vesicles of contacting varicosities is not uniform, but the significance of this observation is not yet known.

The AP axon also gives rise to spinelike projections which are directly contacted by neurites from other peripheral sensory afferents adjacent to their respective neuropils. Figure 18 illustrates a contact adjacent to a target region within the somato-, chemosensory neuropils, the ventral tract. Here, just as in the optic neuropil, the AP cell process does not enter the large bundle of sensory afferent axons and terminals, but instead contacts small groups of sensory afferent nerve terminals at the periphery of the ventral tract. Again, we found that the neuritic contacts from the sensory afferents took two basic forms: circular axon-like, and varicosities with dense accumulation of synaptic vesicles.

Figure 16. Magnified view of the region shown in the box in Figure 15. A spinelike process from the main axon of the AP cell (AP) is directly contacted by photoreceptor processes bearing the surface epitope identified by mAb Lan3-2. In this region of contact, the Lan3-2 labeled neurites are enlarged into irregularly shaped varicosities which contain synaptic vesicles in large numbers. The cytoplasmic appearance and characteristic vesicle type vary from profile to profile. Calibration bar = 0.5 μ m.

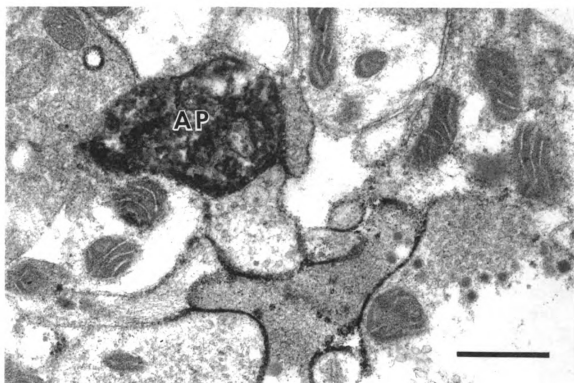
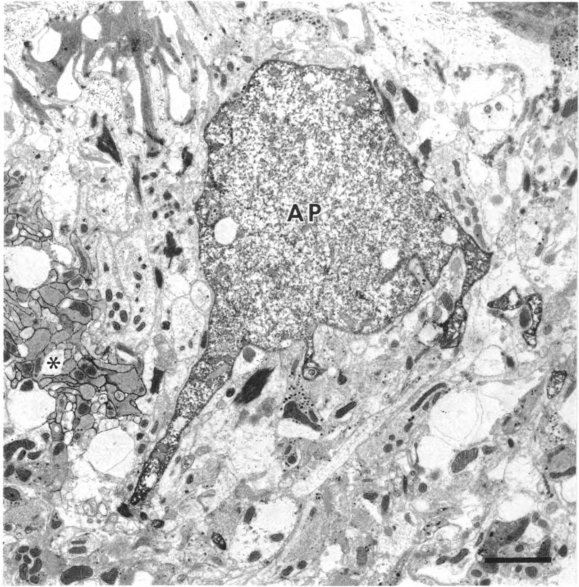


Figure 17. Electron micrograph showing that AP cell projections contact photoreceptors.

In this region, the AP axon (AP, intracellular DAB reaction product) forms frequent, small side branches in the immediate vicinity of the major photoreceptor axon bundle in the optic neuropil (*, surface reaction product). Here, the AP spines are surrounded by photoreceptor neurites which have the cytoplasm characteristic of axons, and which do not appear to be making synapses. TEM section taken approximately halfway between the interganglionic connectives and the anterior nerve root. Calibration bar = 2 μm .

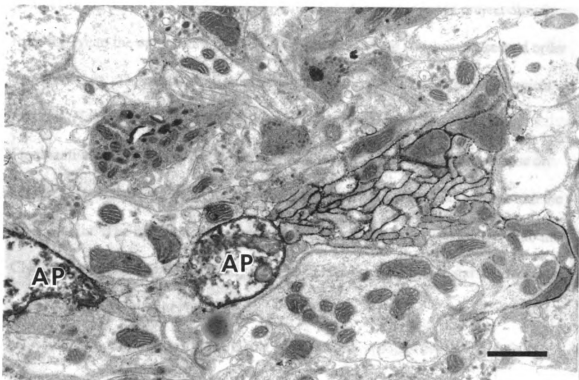


The presence of direct contacts between AP axonal processes and sensory afferents in the optic and the somato-, chemosensory neuropils suggests that the AP cell may function as a second order visual interneuron, as well as an interneuron for other sensory modalities.

Figure 18. Electron micrograph showing that AP cell projections contact somato-, chemosensory neuropils.

TEM cross-section through juvenile midbody ganglion approximately 1/3 of the way between the interganglionic connectives and the anterior nerve root.

Two AP cell projections are visible in this section. One of these (center) is approached by neurites from the adjacent ventral tract. The ventral tract belongs to the large somato-, chemosensory neuropil. AP cell projections are also contacted by non-optic sensory afferents in the more lateral somato-, chemosensory neuropils. Calibration bar = 1 μ m.



DISCUSSION

We have investigated the leech visual system, consisting of photoreceptors located both in the eyes and in the midbody sensilla and some of their second order central neurons in terms of their anatomy and biochemistry using fluorescent and electron dense tracers and antibodies generated against leech antigens.

Injecting diO into leech eyes, we showed that photoreceptor axons project directly from the eye to the optic neuropil of the CNS ganglia, where they contact second order visual neurons. This result confirmed earlier ultrastructural and electrophysiological findings (Hansen, 1962; Röhlich and Török, 1964; Lasansky and Fuortes, 1969; Fioravanti and Fuortes, 1972; Peterson, 1983) that photoreceptors do not synapse on second order visual neurons in the eye, but instead project their primary axons into the CNS ganglia. The invariant, strong staining of axons through the head nerves into the CNS indicates that diO diffused only along the photoreceptor axons, and that they were not dye-coupled with other neurons.

A novel finding we report here is that photoreceptors project their axons into a CNS target region which is separate from those of other sensory neuropils, the optic neuropil. Moreover, we showed that photoreceptor axons do not terminate in the head ganglia but also extend as an optic tract into the interganglionic connectives to innervate the optic neuropils of segmental ganglia. Because optic neuropils and optic tracts can be immunostained in all CNS ganglia, it is likely that some of the photoreceptor axons extend throughout the chain of 32 ganglia which comprise the leech CNS. Also, the optic neuropil of a segmental ganglion consists of a considerably larger number of

photoreceptor axons than could be accounted for by the few sensillar photoreceptors originating in that segment, assuming that photoreceptors share the branching pattern of other sensory afferents in the neuropil, e.g. bifurcation and a limited number of short branchlets emanating from the bifurcated axon (Jellies et al., 1994).

We showed that galectin serves as a specific label for both first order visual neurons, the photoreceptors in the eye and in midbody sensilla. Low levels of galectin appear to be present on the cell surface as suggested by staining live neurons. Galectin is also present in the cytoplasm, as suggested by the homogeneous staining of the photoreceptor cell body in fixed, permeabilized preparation. Galectin is absent from the vacuole, a large compartment in the middle of the cell body, which is connected to the extracellular space through low resistance channels. The galectin-negative, proteinaceous material inside the vacuole is thought to act as the lens for the microvillar membrane (Röhlich and Török, 1964) which delimits the vacuole. This microvillar membrane responds to increases in illumination with increases in conductance (Fioravanti and Fuortes, 1972; Peterson, 1984). Galectin is presumably not involved in the transduction of light because it is present both in the photoreceptor cell body, where generator potentials originate in response to light, but also in the photoreceptor axon which conducts action potentials to the CNS where they provide input to second order visual neurons (Peterson, 1984).

Previously, a number of different CNS neurons were shown to be excited by increases in illumination (Bagnoli et al., 1973; Kretz et al., 1976; Peterson, 1984), among them several neurons that reiterate in most CNS ganglia such as cells 153, 154, the AE and S cells, and a neuron present only in midbody ganglion 1, the lateral visual (LV) cell. So far, only the LV cell has been shown to be a second order visual neuron. Here we provide

light and ultrastructural evidence that other, segmentally reiterated neurons are contacted by photoreceptor axons. Using confocal microscopy, we demonstrated that the large primary axon of the AP cell colocalizes with the optic neuropil. The two effector cells tested, the AE and Retzius cells, do not project primary axons close to the optic neuropil but only thin, secondary processes. The two central neurons tested, the P and N cell only demonstrate a slight degree of colocalization of a few branches with the optic neuropil. In the leech, the technique of illustrating the colocalization of processes of two different types of neurons at the light level has so far reliably led to the identification of monosynaptically connected neurons at the EM level (Macagno et al., 1987).

We confirmed the intimate contact between photoreceptor axons and the AP cell at the ultrastructural level. To be able to easily identify photoreceptor neurites and AP cell processes, we first surface stained live photoreceptor axons with HRP-conjugated Lan3-2 and filled the cytoplasm of the AP cell with dissolved HRP and only subsequently fixed the specimen. It is possible to use a general sensory afferent stain to identify the photoreceptor axons and varicosities at the EM level, because of the considerable distance between the optic neuropil and the somatosensory-, chemosensory neuropils (about 100 μm) into which other sensory modalities project (Zipser, 1994).

Intriguingly, the contacts (both axon-like and varicosities) that we observed between the spines of the AP cell and photoreceptors occur at a distance of about 5 to 10 μm from the major bundle of photoreceptor axons in the optic neuropil. We have not so far observed the AP cell spines entering the photoreceptor axon bundle directly. The 5 to 10 μm distance of AP cell/photoreceptor contact to the larger photoreceptor axon bundle of the optic neuropil corresponds to the distance over which sensory afferents defasciculate

and branch as they project de novo into the synaptic neuropil during early embryogenesis (Zipser et al., 1989; Zipser and Cole, 1991). We previously provided evidence that these short sensory afferent projections occur independently from one another by demonstrating that their disappearance, as a result of antibody perturbation, followed first order kinetics. This has led to the speculation that sensory afferents leave their bundled axon tracts to independently search for their synaptic partners (Song and Zipser, 1995a). Thus, it is interesting that first, these short projections of sensory afferents away from their major axon bundle are preserved in the mature neuropil and second, that they present sites of intimate contact with central neurons, their candidate postsynaptic neurons. Our preliminary observation that the AP cell can be excited by illuminating photoreceptors in the eyes (Tai and Zipser, preliminary data) is consistent with the AP cell being monosynaptically connected to the photoreceptor axons in the optic neuropil.

Our finding that the AP cell is a candidate postsynaptic partner of galectin positive photoreceptor axons will also make it feasible to study the role of lectins and carbohydrates in the formation of synapses. The AP cell is readily identifiable in the leech embryo and has been extensively characterized (Sunderland, 1980; Wolszon et al., 1994; Wolszon et al., 1994; Wolszon et al., 1995).

The physiological role of galectins in the different nervous systems where it has been studied is still unclear. In the rat, high levels of galectin were detected, by immunostaining, in a subset of sensory afferent neurons projecting into lamina II of the posterior horn and in ventral horn motor neurons. The same sensory neurons, but not the motor neurons, also express galactose-containing glycoconjugates, potential receptors for galectin. Using the more sensitive method of *in situ* hybridization, galectin mRNA was

detected in all sensory afferents. This finding led to the speculation that galectin plays a role in axonal fasciculation and in axonal targeting across the extracellular matrix (Regan et al., 1986; Hynes, 1990). Recent experiments, conducted *in vitro*, supported this hypothesis by demonstrating that galectin L-14 promotes primary olfactory neuron adhesion to laminin as well as intercellular adhesion among olfactory neurons (Mahanthappa et al., 1994). Additional evidence for a role of galectin in axonal fasciculation was found in cultured neural crest cells (Milos et al., 1989). Galectin presumably has different functions because it can be expressed by different cell types, neurons, non-neuronal cell in olfactory nerves (Mahanthappa et al., 1994) and epithelial cells (Hynes et al., 1990; Regan et al., 1986; Cole and Zipser, 1994b).

Perhaps galectin will turn out to mediate several different functions in the leech system. If photoreceptor axons use their high levels of galectin in targeting, it is not yet clear where their corresponding galactose-containing ligands are located. We have not yet identified a galactose-containing marker on the AP cell which could serve as a counterreceptor for galectin. The neurons for which we have so far identified galactose-containing surface markers are sensory afferents conveying mechano-, and chemosensation (Zipser et al., 1994). Preliminary immunostaining suggests that central neurons may contain low levels of galectin (Zipser, unpublished), an observation which will have to be confirmed using *in situ* hybridization. If central neurons were to express low levels of galectin, they might also interact with mechano- and chemodetector neurons that use galactose-containing surface markers in their targeting (Song and Zipser, 1995b; Zipser, 1995). Some of these issues may be addressed using purified galectin or Fab fragments to galectin as reagents in perturbation assays similar as those previously

performed to establish the function of neuronal carbohydrate markers (Song and Zipser, 1995a, b).

The existence of different galectin species in a given organism also speaks for galectin exercising different functions. Throughout phylogeny, galectins are found to occur as 3 different molecular weight forms (about 10 to 20, 30 to 40 or 60 to 70 kD). In the rat, different neurons were shown to express different types of galectins, e.g. sensory afferents express RL16 and RL35 while motor neurons only express RL16. In the leech system, we have not yet been able to determine which galectin forms are expressed by photoreceptor neurons because our antiserum cross reacts with both a 35 kD form (LL35) and a 16 kD form (LL16) (Cole and Zipser, 1994a, b).

In addition to being the only neurons in leech that express high levels of galectin, photoreceptors are also the only neurons found so far to possess the homeotic gene *Lox 6* (Shankland et al., 1991; Wong et al., 1995) which is most homologous to *Drosophila Dfd* (Shankland et al., 1991). The function of *Lox 6* in the leech eyes is not yet known. Thus, leech photoreceptor neurons appear to be a useful model system to study the physiological function of a number of developmentally important molecules.

SUMMARY AND CONCLUSIONS

To study carbohydrate recognition in the nervous system, our lab developed a method for culturing the leech embryos virtually intact. Specific carbohydrate markers on surface glycoproteins, which are expressed by sensory afferent neurons have been characterized through the use of monoclonal antibodies. Our studies demonstrated the developmental functions of these carbohydrate markers. A constitutive mannose-containing marker expressed by the full set of sensory afferents mediates an early step in axonal targeting by allowing sensory afferents to defasciculate and branch as they enter the synaptic neuropil. Ultrastructural analysis demonstrated that this mannose-specific recognition mediates two aspects of synaptogenesis of leech sensory afferents, collateral branching and the formation of synaptic vesicle clusters. Other steps in axonal targeting are mediated by developmentally regulated carbohydrate markers which contain galactose. The galactose-containing markers are specific for subsets of sensory afferents. These subset markers were shown to mediate the consolidation of their respective subsets into appropriate regions of the CNS where it contacts its synaptic partners. Further ultrastructural analysis is needed to understand whether subset carbohydrate markers also mediate synaptogenesis.

Carbohydrates on the cell surface may interact homotypically or heterotypically with carbohydrate binding proteins or lectins. Three leech lectins, LL63, 35 and 16 have been isolated and characterized. LL35 and LL16 are present in the nervous system. They are the putative receptors for the carbohydrate markers. LL35 is expressed abundantly on a small subset of sensory afferent axons which project in the bilateral sensory midline tract

(Cole and Zipser, 1994b). We identified this small subset of sensory afferents as photoreceptors. A central neuron, the AP cell projects its primary axon alongside the optic tract. Because of its intimate contact with the optic tract, the AP cell is a strong candidate second order visual neuron. Thus, leech photoreceptors and their postsynaptic partner provide a simple visual system for studying carbohydrate recognition in the developing nervous system.

LIST OF REFERENCES

LIST OF REFERENCES

- Ashwell, G. and Harford, J. (1982) Carbohydrate-specific receptors of the liver. *Annu. Rev. Biochem.* 51: 531-554.
- Avrameas, S. and Ternynck, T. (1971) Peroxidase labeled antibody and Fab conjugates with enhanced intracellular penetration. *Immunocytochemistry* 8: 1175-1179.
- Bagnoli, P., Brunelli, M., and Magni, F. (1973) Afferent connections to the fast conducting pathway in the central nervous system of the leech. *Arch. Ital. Biol.* 3: 58-75.
- Bajt, M. L., Cole, R. N., and Zipser, B. (1990) The specificity of 130-kDa leech sensory afferent proteins is encoded by their carbohydrate epitopes. *J. Neurochem.* 55(6): 2117-2125.
- Barakat, I., Bezamahouta, C., Zanetta, J. P., and Vincendon, G. (1989) Differential expression of 240 kDa ConA-binding glycoprotein in vitro and in vivo detected by immunochemical methods. *Biol. Cell* 66(3): 317-326.
- Bastmeyer, M. and O'Leary, D. D. (1996) Dynamics of target recognition by interstitial axon branching along developing cortical axons. *J. Neurosci.* 16(4): 1450-1459.
- Baum, P. D. and Garriga, G. (1997) Neuronal migrations and axon fasciculation are disrupted in *ina-1* integrin mutants. *Neuron* 19: 51-62.
- Bleil, J. D. and Wassarman, P. M. (1980) Mammalian sperm-egg interaction: identification of a glycoprotein in mouse egg zonae pellucidae possessing receptor activity for sperm. *Cell* 20(3): 873-882.
- Bradford, M. M. (1976) A rapid and sensitive method for the quantitation of microgram quantities of protein utilizing the principle of protein-dye binding. *Anal. Biochem.* 72: 248-254.
- Braun, J. and Stent, G. S. (1989) Axon outgrowth along segmental nerves in the leech. II. Identification of actual guidance cells. *Dev. Biol.* 132(2): 486-501.
- Cole, R. N. and Zipser, B. (1994a) Carbohydrate-binding proteins in the leech: I. Isolation and characterization of lactose-binding proteins. *J. Neurochem.* 63: 66-74.

- Cole, R. N. and Zipser, B. (1994b) Carbohydrate-binding proteins in the leech: II. Lactose-binding protein LL35 is located to neuronal and muscle subsets and all epithelial cells. *J. Neurochem.* 63: 75-85.
- Dammer, U., Popescu, O., Wagner, P., Anselmetti, D., Guntherodt, H. J., and Misevic, G. N. (1995) Binding strength between cell adhesion proteoglycans measured by atomic force microscopy. *Science* 267(5201): 1173-1175.
- Daston, M. M., Bastmeyer, M., Rutishauser, U., and O'Leary, D. D. (1996) Spatially restricted increase in polysialic acid enhances corticospinal axon branching related to target recognition and innervation. *J. Neurosci.* 16(17): 5488-5497.
- Dodd, J. and Jessell, T. M. (1986) Cell surface glycoconjugates and carbohydrate-binding proteins: possible recognition signals in sensory neuron development. *J. Exp. Biol.* 124: 225-238.
- Drickamer, K. (1988) Two distinct classes of carbohydrate-recognition domains in animal lectins. *J. Biol. Chem.* 263(20): 9557-9560.
- Elliott, E. J. (1987) Morphology of chemosensory organs required for feeding in the leech *Hirudo medicinalis*. *J. Morphol.* 192(2): 181-187.
- Faissner, A., Clement, A., Lochter, A., Streit, A., Mandl, C., and Schachner, M. (1994) Isolation of a neural chondroitin sulfate proteoglycan with neurite outgrowth promoting properties. *J Cell Biol* 126(3): 783-799.
- Fernandez, J. and Stent, G. S. (1982) Embryonic development of the hirudinid leech *Hirudo medicinalis*: structure, development and segmentation of the germinal plate. *J. Embryol. Exp. Morphol.* 72: 71-96.
- Fioravanti, R. and Fuortes, M. G. (1972) Analysis of responses in visual cells of the leech. *J. Physiol. Lond.* 227(1): 173-194.
- Flaster, M. S., Schley, C., and Zipser, B. (1983) Generating monoclonal antibodies against excised gel bands to correlate immunocytochemical and biochemical data. *Brain Res.* 277(1): 196-199.
- Gallatin, M., St. John, T. P., Siegelman, M., Reichert, R., Butcher, E. C., and Weissman, I. L. (1986) Lymphocyte homing receptors. *Cell* 44(5): 673-680.
- Grumet, M., Flaccus, A., and Margolis, R. U. (1993) Functional characterization of chondroitin sulfate proteoglycans of brain: interactions with neurons and neural cell adhesion molecules. *J. Cell. Biol.* 120(3): 815-824.

- Halloran, M. C. and Kalil, K. (1994) Dynamic behaviors of growth cones extending in the corpus callosum of living cortical brain slices observed with video microscopy. *J. Neurosci.* 14(4): 2161-2177.
- Hansen, K. (1962) Elektronenmikroskopische Untersuchung der Hirudineen-Augen. *Zool. Beitr.* 7: 83-128.
- Harlow, E. and Lane, D. (1988) *Antibodies: A laboratory manual.* Cold Spring Harbor, NY, Cold Spring Harbor laboratory.
- Harris, W. A., Holt, C. E., and Bonhoeffer, F. (1987) Retinal axons with and without their somata, growing to and arborizing in the tectum of *Xenopus* embryos: a time-lapse video study of single fibers in vivo. *Development* 101(1): 123-133.
- Heiland, P. C., Griffith, L. S., Lange, R., Schachner, M., Hertlein, B., Traub, O., and Schmitz, B. (in press) Tyrosine and serine phosphorylation of the neural cell adhesion molecule L1 is implicated in its oligomannosidic glycan dependent association with NCAM and neurite outgrowth. *Eur. J. Cell Biol.*
- Hirabayashi, J., Ubukata, T., and Kasai, K. (1996) Purification and molecular characterization of a novel 16-kDa galectin from the nematode *Caenorhabditis elegans*. *J. Biol. Chem.* 271(5): 2497-2505.
- Hogg, N., Flaster, M., and Zipser, B. (1983) Cross-reactivities of monoclonal antibodies between select leech neuronal and epithelial tissues. *J. Neurosci. Res.* 9(4): 445-457.
- Horstkorte, R., Schachner, M., Magyar, J. P., Vorherr, T., and Schmitz, B. (1993) The fourth immunoglobulin-like domain of NCAM contains a carbohydrate recognition domain for oligomannosidic glycans implicated in association with L1 and neurite outgrowth. *J Cell Biol* 121(6): 1409-1421.
- Huang, Y., Jellies, J., Johansen, K. M., and Johansen, J. (1997) Differential glycosylation of tractin and leechCAM, two novel Ig superfamily members, regulates neurite extension and fascicle formation. *J. Cell. Biol.* 138: 143-157.
- Hynes, M. A., Gitt, M., Barondes, S. H., Jessell, T.M. and Buck, L. B. (1990) Selective expression of an endogenous lactose-binding lectin gene in subsets of central and peripheral neurons. *J. Neurosci.* 10(3): 1004-1013.
- Inoue, A. and Sanes, J. R. (1997) Lamina-specific connectivity in the brain: regulation by N-cadherin, neurotrophins, and glycoconjugates. *Science* 276(5317): 1428-1431.
- Itoh, K., Konishi, A., Nomura, S., Mizuno, N., Nakamura, Y., and Sugimoto, T. (1979) Application of coupled oxidation reaction to electron microscopic demonstration of

- horseradish peroxidase: cobalt-glucose oxidase method. *Brain Res.* 175(2): 341-346.
- Jellies, J., Johansen, K., and Johansen, J. (1994) Specific pathway selection by the early projections of individual peripheral sensory neurons in the embryonic medicinal leech. *J. Neurobiol.* 25(10): 1187-1199.
- Jessell, T. M., Hynes, M. A., and Dodd, J. (1990) Carbohydrates and carbohydrate-binding proteins in the nervous system. *Annu. Rev. Neurosci.* 13: 227-255.
- Johansen, K. M., Kopp, D. M., Jellies, J., and Johansen, J. (1992) Tract formation and axon fasciculation of molecularly distinct peripheral neuron subpopulations during leech embryogenesis. *Neuron* 8(3): 559-572.
- Kaethner, R. J. and Stuermer, C. A. (1992) Dynamics of terminal arbor formation and target approach of retinotectal axons in living zebra fish embryos: a time-lapse study of single axons. *J. Neurosci.* 12(8): 3257-3271.
- Kasai, K. (1990) Biochemical properties of vertebrate 14K bean-galactoside-binding lectins. New York, Springer-Verlag.
- Kornfield, R. and Kornfield, S. (1985) Assembly of asparagine-linked oligosaccharides. *Ann. Rev. Biochem.* 54: 631-664.
- Kretz, J. R., Stent, G. S., and Kristan, W. B. (1976) Photosensory input pathways in the medicinal leech. *J. Comp. Physiol.* 106: 1-37.
- Landmesser, L., Dahm, L., Tang, J. C., and Rutishauser, U. (1990) Polysialic acid as a regulator of intramuscular nerve branching during embryonic development. *Neuron* 4(5): 655-667.
- Lasansky, A. and Fuortes, M. G. (1969) The site of origin of electrical responses in visual cells of the leech, *Hirudo medicinalis*. *J. Cell Biol.* 42(1): 241-252.
- Macagno, E. R., Muller, K. J., and Pitman, R. M. (1987) Conduction block silences parts of a chemical synapse in the leech central nervous system. *J. Physiol. Lond.* 387: 649-664.
- Mahanthappa, N. K., Cooper, D. N., Barondes, S. H., and Schwarting, G. A. (1994) Rat olfactory neurons can utilize the endogenous lectin, L-14, in a novel adhesion mechanism. *Development* 120(6): 1373-1384.
- Martin, P. T. and Sanes, J. R. (1995) Role for a synapse-specific carbohydrate in agrin-induced clustering of acetylcholine receptors. *Neuron* 14(4): 743-754.

- McGlade-McCulloh, E., Muller, K. J., and Zipser, B. (1990) Expression of surface glycoproteins early in leech neural development. *J. Comp. Neurol.* 299(1): 123-131.
- Milos, N. C., Ma, Y. L., and Frunchak, Y. N. (1989) Involvement of endogenous galactoside-binding lectin of *Xenopus laevis* in pattern formation of *Xenopus* neurites in vitro. *Cell Differ. Dev.* 28(3): 203-209.
- Misevic, G. N. and Burger, M. M. (1993) Carbohydrate-carbohydrate interactions of a novel acidic glycan can mediate sponge cell adhesion. *J. Biol. Chem.* 268(7): 4922-4929.
- Nakamura, H. and O'Leary, D. D. (1989) Inaccuracies in initial growth and arborization of chick retinotectal axons followed by course corrections and axon remodeling to develop topographic order. *J. Neurosci.* 9(11): 3776-3795.
- O. Rourke, N. A., Cline, H. T., and Fraser, S. E. (1994) Rapid remodeling of retinal arbors in the tectum with and without blockade of synaptic transmission. *Neuron* 12(4): 921-934.
- Oudega, M., Marani, E., and Thomeer, R. T. (1992) Transient expression of stage-specific embryonic antigen-1 (CD15) in the developing dorsal rat spinal cord. *Histochem. J.* 24(11): 869-877.
- Peinado, A., Macagno, E. R., and Zipser, B. (1987) A group of related surface glycoproteins distinguish sets and subsets of sensory afferents in the leech nervous system. *Brain Res.* 410: 335-339.
- Peinado, A., Zipser, B., and Macagno, E. R. (1990) Segregation of afferent projections in the central nervous system of the leech *Hirudo medicinalis*. *J. Comp. Neurol.* 301: 232-242.
- Peterson, E. L. (1983) Visual processing in the leech central nervous system. *Nature* 303(5914): 240-242.
- Peterson, E. L. (1984) Photoreceptors and visual interneurons in the medicinal leech. *J. Neurobiol.* 15(6): 413-428.
- Pfeifer, K., Haasemann, M., Gamulin, V., Bretting, H., Fahrenholz, F., and Muller, W. E. (1993) S-type lectins occur also in invertebrates: high conservation of the carbohydrate recognition domain in the lectin genes from the marine sponge *Geodia cydonium*. *Glycobiology* 3(2): 179-184.

- Pfenninger, K. H., Maylie-Pfenninger, M. F., Friedman, L. B., and Simkowitz, P. (1984) Lectin labeling of sprouting neurons. III. Type-specific glycoconjugates on growth cones of different origin. *Dev. Biol.* 106(1): 97-108.
- Phillips, C. E. and Friesen, W. O. (1982) Ultrastructure of the water-movement-sensitive sensilla in the medicinal leech. *J. Neurobiol.* 13(6): 473-486.
- Puche, A. C., Poirier, F., Hair, M., Bartlett, P. F., and Key, B. (1996) Role of galectin-1 in the developing mouse olfactory system. *Dev Biol* 179(1): 274-287.
- Regan, L. J., Dodd, J., Barondes, S. H., and Jessell, T. M. (1986) Selective expression of endogenous lactose-binding lectins and lactoseries glycoconjugates in subsets of rat sensory neurons. *Proc. Natl. Acad. Sci. USA* 83: 2248-2252.
- Riddle, D. R., Wong, L. D., and Oakley, B. (1993) Lectin identification of olfactory receptor neuron subclasses with segregated central projections. *J. Neurosci.* 13(7): 3018-3033.
- Röhlich, P. and Török, L. J. (1964) Elektronenmikroskopische Beobachtungen an den Sehzellen des Blutegels, *Hirudo medicinalis*. *L. Zeitschrift für Zellforschung* 63: 618-635.
- Rosen, S. D., Singer, M. S., Yednock, T. A., and Stoolman, L. M. (1985) Involvement of sialic acid on endothelial cells in organ-specific lymphocyte recirculation. *Science* 228(4702): 1005-1007.
- Rutishauser, U., Acheson, A., Hall, A. K., Mann, D. M., and Sunshine, J. (1988) The neural cell adhesion molecule (NCAM) as a regulator of cell-cell interactions. *Science* 240(4848): 53-57.
- Sanes, J. R. and Cheney, J. M. (1982) Lectin binding reveals a synapse-specific carbohydrate in skeletal muscle. *Nature* 300(5893): 646-647.
- Scott, L. J., Bacou, F., and Sanes, J. R. (1988) A synapse-specific carbohydrate at the neuromuscular junction: association with both acetylcholinesterase and a glycolipid. *J. Neurosci.* 8(3): 932-944.
- Scott, L. J., Balsamo, J., Sanes, J. R., and Lilien, J. (1990) Synaptic localization and neural regulation of an N-acetylgalactosaminyl transferase in skeletal muscle. *J. Neurosci.* 10(1): 346-350.
- Scott, S. A., Patel, N., and Levine, J. M. (1990) Lectin binding identifies a subpopulation of neurons in chick dorsal root ganglia. *J. Neurosci.* 10(1): 336-345.

- Shankland, M., Martindale, M. Q., Nardelli-Haeffliger, D., Baxter, E., and Price, D. J. (1991) Origin of segmental identity in the development of the leech nervous system. *Development Suppl* 2: 29-38.
- Sharon, N. and Lis, H. (1989) Lectins as cell recognition molecules. *Science* 246(4927): 227-234.
- Sharon, N. and Lis, H. (1993) Carbohydrates in cell recognition. *Sci. Am.* 268(1): 82-89.
- Simon, D. K. and O'Leary, D. D. (1990) Limited topographic specificity in the targeting and branching of mammalian retinal axons. *Dev. Biol.* 137(1): 125-134.
- Snow, D. M., Watanabe, M., Letourneau, P. C., and Silver, J. (1991) A chondroitin sulfate proteoglycan may influence the direction of retinal ganglion cell outgrowth. *Development* 113(4): 1473-1485.
- Sokal, R. R. and Rohlf, F. J. (1981) *Biometry*. San Francisco, CA, W. H. Freeman and Company.
- Solter, D. and Knowles, B. B. (1978) Monoclonal antibody defining a stage-specific mouse embryonic antigen (SSEA-1). *Proc. Natl. Acad. Sci. USA* 75(11): 5565-5569.
- Song, J. and Zipser, B. (1995a) Kinetics of the inhibition of axonal defasciculation and arborization mediated by carbohydrate markers in the embryonic leech. *Dev. Biol.* 168: 319-331.
- Song, J. and Zipser, B. (1995b) Targeting of neuronal subsets mediated by their sequentially expressed carbohydrate markers. *Neuron* 14: 537-547.
- Sunderland, A. J. (1980) A hitherto undocumented pair of neurons in the segmental ganglion of the leech which receives synaptic input from mechanosensory cells. *Comp. Biochem. Physiol.* 67A: 299-302.
- Tai, M.-H., Rheuben, M. B., Autio, D. M., and Zipser, B. (1996) Leech photoreceptors project their galectin-containing processes into the optic neuropils where they contact AP cells. *J. Comp. Neurol.* 371(2): 235-248.
- Takeichi, M. (1986) *Molecular basis for teratocarcinoma cell-cell adhesion*. New York, Plenum.
- Ungersbock, A., Kretz, R., and Rager, G. (1991) Synaptogenesis in the primary visual cortex of the tree shrew (*Tupaia belangeri*). *J. Comp. Neurol.* 308(3): 491-504.

- Varki, A. (1993) Biological roles of oligosaccharides: all of the theories are correct. *Glycobiology* 3(2): 97-130.
- Wang, H. and Macagno, E. R. (1997) The establishment of peripheral sensory arbors in the leech: *in vivo* time-lapse studies reveal a highly dynamic process. *J. Neurosci.* 17: 2408-2419.
- Wassarman, P. M. (1987) Early events in mammalian fertilization. *Annu. Rev. Cell. Biol.* 3: 109-142.
- Weisblat, D. A. and Shankland, M. (1985) Cell lineage and segmentation in the leech. *Philos. Trans. R. Soc. Lond. B. Biol. Sci.* 312(1153): 39-56.
- Wolszon, L. R., Gao, W. Q., Passani, M. B., and Macagno, E. R. (1994) Growth cone "collapse" *in vivo*: are inhibitory interactions mediated by gap junctions? *J. Neurosci.* 14(3 Pt 1): 999-1010.
- Wolszon, L. R., Passani, M. B., and Macagno, E. R. (1995) Interactions during a critical period inhibit bilateral projections in embryonic neurons. *J. Neurosci.* 15(2): 1506-1515.
- Wolszon, L. R., Rehder, V., Kater, S. B., and Macagno, E. R. (1994) Calcium wave fronts that cross gap junctions may signal neuronal death during development. *J. Neurosci.* 14(6): 3437-3448.
- Wong, V. Y., Aisemberg, G. O., Gan, W. B., and Macagno, E. R. (1995) The leech homeobox gene *Lox4* may determine segmental differentiation of identified neurons. *J. Neurosci.* 15(8): 5551-5559.
- Wulf, J. (1982) Sensitivity changes of photoreceptor cells of *Hirudo medicinalis* caused by changes in extracellular calcium concentration. *Biophys Struct. Mech.* 8(3): 173-187.
- Yoshihara, M., Rheuben, M. B., and Kidokoro, Y. (1997) Transition from growth cone to functional motor nerve terminal in *Drosophila* embryos. *J. Neurosci.* 17(21): 8408-8426.
- Zipser, B. and Cole, R. N. (1991) A mannose-specific recognition mediates the defasciculation of axons in the leech CNS. *J. Neurosci.* 11(11): 3471-3480.
- Zipser, B. and McKay, R. (1981) Monoclonal antibodies distinguish identifiable neurons in the leech. *Nature* 289(5798): 549-554.
- Zipser, B., Morell, R., and Bajt, M. L. (1989) Defasciculation as a neuronal pathfinding strategy: Involvement of a specific glycoprotein. *Neuron* 3: 621-630.

Zipser, K., Erhardt, M., Song, J., Cole, R. N. and Zipser, B. (1994) Distribution of carbohydrate epitopes among disjoint subsets of leech sensory afferent neurons. *J. Neurosci.* 14(7): 4481-4493.

MICHIGAN STATE UNIV. LIBRARIES



31293017665054